

1 The causal connections between gut microbiota and chronic pain and pain
2 phenotypes through the gut-brain axis: A Mendelian randomization study
3 and mediation analysis

4

5 Jia Chen^{#ab}, MD, Xuemei Luo^{#ab}, BD, Luyao Wang^{ab}, MD, Yiping Luo^{ab},
6 MD, Xia Deng^{ab}, MD, Yuan Tian^{ab}, MD, Qiao Lu^{ab}, BD, Genwen Sun^{ab},
7 MD, Michael Maes^{*ab}, MD, PhD, Xu Zhang^{*ab}, PhD

8

9 a:Sichuan Provincial Center for Mental Health, Sichuan Provincial
10 People's Hospital, School of Medicine, University of Electronic Science
11 and Technology of China, Chengdu 610072, China.

12 b:Key Laboratory of Psychosomatic Medicine, Chinese Academy of
13 Medical Sciences, Chengdu, 610072, China.

14 #:Co-first author

15 *:First Corresponding author (Xu Zhang)

16 Email:26867455@qq.com

17 * : Co-Corresponding author (Michael Maes)

18 Email:dr.michaelmaes@hotmail.com

19

20 Author contributions

21 Xu Zhang, Michael Maes, Xuemei Luo, and Jia Chen contributed to study
22 design, data acquisition and analysis, manuscript drafting and revision,

23 and the supervision of the research. Luyao Wang, Yiping Luo, Yuan Tian
24 and Xia Deng contributed to the data analysis and manuscript revision,
25 Qiao Lu and Genwen Sun contributed to the manuscript revision. All
26 authors reviewed and approved the paper for publication.

27

28 Acknowledgements

29 We wish to acknowledge the participants and investigators of the UK
30 Biobank, FINRISK 2002 study, Enhancing NeuroImaging Genetics
31 through Meta-Analysis Consortium, the Integrative Epidemiology Unit
32 (IEU, <https://gwas.mrcieu.ac.uk/>), the GWAS Catalog
33 (<https://www.ebi.ac.uk/gwas/>).

34

35 Funding

36 No funding was received for this research.

37

38 Declaration of competing interest

39 None declared.

40

41 Competing interests

42 The authors declare that the research was conducted in the absence of any
43 commercial or financial relationships that could be construed as a
44 potential conflict of interest.

45

46 Data availability

47 All relevant data are within the manuscript and its Supplementary

48 Material.

49

50

51 Abstract

52 Recent studies have increasingly highlighted a potential link between gut
53 microbiota (GM) and chronic pain. However, existing research has
54 yielded mixed results, leaving many questions unanswered. We employed
55 a two-sample Mendelian randomization design to investigate whether
56 GM directly influences multisite chronic pain (MCP) and eight
57 phenotypes. We then used a combination of meta-analysis, genetic
58 colocalization analysis, and Bayesian weighted mendelian randomization
59 to further strengthen the evidence for causal relationship. Additionally,
60 we examined how GM might be associated with human brain structures.
61 Finally, we used mediation analysis to explore whether the structure and
62 function of specific brain regions play a role in the relationship between
63 GM and MCP and the pain phenotypes.

64 We observed a significant causal association between 13 GM and chronic
65 pain. Eight GM protected against pain phenotypes, whereas seven
66 increased risk. The results indicate that GM could potentially affect the
67 area, thickness, and volume of brain region cortices involved in sensory,
68 emotional, and cognitive aspects of pain. Importantly, our findings
69 indicated that the causal effect between the Genus *Odoribacter* and
70 neck/shoulder pain could be mediated by the mean optical density in the
71 left Fornix cres+Stria terminalis. In conclusion, different pain phenotypes
72 were causally associated with different GM among European ancestry.

73 Core GM may influence chronic pain by affecting complex brain
74 networks. Notably, we constructed a basic gut-brain axis model for
75 neck/shoulder pain, involving the Genus *Odoribacter*, left Fornix
76 cres+Stria terminalis, and neck/shoulder pain.

77

78 Key words: chronic pain, pain phenotype, Gut microbiota, Gut-brain axis,
79 Brain imaging, metagenomics

80

81

82 Introduction

83 Chronic pain (CP) is a major public health issue with significant global
84 attention. About 30% global population experiences CP [34]. While
85 various causes exist, CP can be idiopathic (with unknown origin) or
86 difficult to categorize pathophysiologically [82]. Notably, CP shows a
87 genetic link, with pain phenotypes exhibiting heritability [49].

88 The gut microbiota (GM) is the human body's most complex and densely
89 populated microbial ecosystem [33,76]. Recent research highlights its
90 emerging role in the pathophysiology and regulation of pain [62-63]. The
91 gut-brain axis (GBA) is a complex network of communication channels
92 between the gut and brain [66], disruptions in which might be linked to
93 neurological diseases including pain [27, 66].

94 Preclinical studies have demonstrated a link between GM and visceral
95 pain [25,53]. Probiotics can lessen visceral pain [80] and might even
96 affect the development of brain regions involved in pain processing [45].
97 Animal studies further suggest that GM influences various chronic pain
98 conditions, including pain caused by inflammation and nerve damage [40,
99 62]. Other findings hint at a possible connection to nociceptive pain,
100 complex regional pain syndrome, and headaches [50]. This suggests that
101 GM might directly or indirectly regulate neuronal excitability in the
102 peripheral nervous system [61-62, 74].

103 Despite these findings, the causal effect of GM on pain remains unclear

104 due to potential biases. Mendelian randomization (MR) has been
105 employed to investigate the relationship between GM and specific pain
106 conditions, including colorectal cancer [39], irritable bowel syndrome
107 [42], intervertebral disc degeneration [22], osteoarthritis [38,94],
108 ankylosing spondylitis [90], and back pain [29,78]. Not only are the
109 conclusions of the above-mentioned studies inconsistent, but also pain
110 with unclear pathophysiology is more common in clinical practice. This
111 underscores the need to examine pain phenotypes.

112 While the microbiota's role in pain is gaining traction, many questions
113 remain unanswered. In chronic pain, key questions include whether the
114 GM plays a role in chronic pain and different pain phenotypes? How can
115 GBA models be constructed for chronic pain and different pain
116 phenotypes? MR can analyze the potential causal relationship between
117 GM and pain by using genetic variations as instrumental variables (IVs)
118 [37]. Furthermore, mediation analysis [67] can help decompose the
119 impact of GM on pain.

120 In this study, we aimed to (1) identify potential positive GM affecting
121 multisite chronic pain (MCP) and eight pain phenotypes, (2) analyze the
122 effect of potential positive GM on brain structure, and (3) develop a basic
123 GBA model for MCP and pain phenotypes to provide practical
124 suggestions for clinical practice.

125

126 Materials and methods

127 1.1 Study design

128 This study investigated the potential cause-and-effect link between GM
129 and chronic pain using a two-sample MR approach. We utilized data on
130 four relevant GM features and assessed their association with both MCP
131 and eight specific pain phenotypes. We further evaluated the relationship
132 between positive exposure and outcomes using meta-analysis and genetic
133 colocalization analysis. Subsequently, we examined the relationship
134 between potential positive GM and brain imaging-derived phenotypes,
135 and brain structure. Finally, we explored whether the structure and
136 function of specific brain regions impacted the relationship between
137 positive GM and MCP, as well as the eight pain phenotypes, through
138 mediation analysis.

139

140 1. Data sources and instruments

141 To minimize bias caused by sample overlap, we obtained exposure (GM)
142 and outcome (MCP and pain phenotype) data from independent sources.
143 Table 1 summarizes the data sources and sample sizes. Ethical approval
144 for the original studies was publicly confirmed, and this analysis did not
145 require separate ethical approval.

146

147 2.1 MCP

148 We obtained data on MCP from the UK Biobank Consortium, a large
149 collection of genetic and health information. This database includes
150 genome-wide association studies (GWAS) for a large population of
151 European ancestry (387,649 individuals) [31]. MCP referred to chronic
152 pain lasting 3 months or more in the head, face, neck/shoulder, back,
153 stomach/abdomen, hip, and knee.

154

155 2.2 Eight pain phenotypes

156 Data on eight individual pain conditions were collected from UK Biobank
157 participants (ranging from 151,922 to 226,683 participants depending on
158 the specific pain type) [49]. A validated questionnaire was utilized to
159 assess participants' experiences with pain in the past month that impacted
160 their daily activities, including pain in the head, face, neck/shoulder pain,
161 back, stomach/abdomen, hips, knees, and all over the body. We excluded
162 participants who chose "prefer not to say" and focused on pain in seven
163 specific locations (head, neck/shoulder, back, abdomen, face, knee, and
164 hip). Individuals who reported pain in a specific location were classified
165 as cases, regardless of other pain selections. Participants who reported
166 "none of the above" were classified as controls. We also included "pain
167 all over the body" as a potential indicator of chronic widespread pain,
168 which is a distinct condition from localized chronic pain.

169

170 2.3 GM

171 Data 1: MiBioGen consortium study (14,306 Europeans): This study used
172 16S rRNA gene sequencing and analyzed 211 microbial taxa (9 phyla, 16
173 classes, 20 orders, 35 families, 131 genera) from European
174 participants[36].

175 Data 2: German single-country GWAS study (8,956 Germans): This study
176 analyzed gut bacteria using 16S rRNA gene sequencing[65]. We
177 examined 233 different bacterial groups (4 phyla, 8 classes, 6 orders, 10
178 families, 29 genera; 65, 62, and 49 at 97% OTU, 99% OTU, and ASV
179 levels) to understand their abundance. Additionally, we analyzed the
180 presence or absence of 198 bacterial features (2 classes, 1 order, 2
181 families, 17 genera; 65, 62, and 49 on 97% OTU, 99% OTU, and ASV
182 levels), based on taxonomic annotation or ASV/OTU clustering.

183 Data 3: Dutch Microbiome Project study (7,738 individuals): This study
184 used shotgun metagenomic sequencing[44] and analyzed 207 microbial
185 taxa (5 phyla, 10 classes, 13 orders, 26 families, 48 genera, and 105
186 species) and 205 functional pathways.

187 Data 4: FINRISK 2002 study (5,959 individuals): This study used
188 shotgun metagenomic sequencing [60] and analyzed 471 distinct Genome
189 Taxonomy Database (GTDB) taxa (11 phyla, 19 classes, 24 orders, 62
190 families, 146 genera, and 209 species).

191

192 2.4 Brain

193 2.4.1 Brain imaging-derived phenotypes

194 Summary statistics for brain imaging-derived (BID) phenotypes were
195 obtained from a large GWAS conducted by Smith et al. [70] using data
196 from the UK Biobank, which included 39,691 European individuals. This
197 dataset comprises nearly 4,000 BID phenotypes encompassing brain
198 structure, function, connectivity, and microstructure.

199

200 2.4.2 Human brain cortical data

201 We leveraged brain magnetic resonance imaging (MRI) data from a
202 large-scale analysis (genome-wide association meta-analysis) involving
203 over 51,000 individuals of European descent across 60 separate studies.
204 This analysis was conducted by a research group within the Enhancing
205 NeuroImaging Genetics through Meta-Analysis (ENIGMA) Consortium.
206 The study focused on two key aspects of the brain's outer layer (cortex):
207 the total surface area (SA) and average thickness (TH). Additionally, they
208 examined 34 specific regions within the cortex known to have distinct
209 functions, as defined by the Desikan-Killiany atlas [24]. For further
210 details, please refer to the original ENIGMA study. In our analysis, we
211 specifically used data on the SA and TH of these brain regions,
212 accounting for overall brain size and genetic background.

213

214 2.4.3 Brain-wide volumes

215 Researchers developed a technique called genomic principal component
216 analysis (PCA), which allowed them to analyze brain scans and identify
217 general underlying patterns in brain structures (morphometry) across the
218 entire brain; the analysis takes into account the potential underlying
219 genetic influences [21]. This technique was applied to genetic data
220 associated with 83 distinct brain volume measurements in over 36,000
221 UK Biobank participants. Unlike traditional methods that focus on
222 genetic similarity between individuals, Genomic PCA identifies key
223 genetic components that capture the overall variation in brain volume
224 across different brain regions.

225

226 3. Genetic variants selection criteria

227 We identified genetic variations (single nucleotide polymorphisms, SNPs)
228 that strongly influence GM using strict criteria, including a very low
229 P-value ($<1 \times 10^{-5}$) [78], a 10000-kb window around a leading SNP, and
230 minimal linkage disequilibrium (LD, $r^2 < 0.001$, kb=10000) with other
231 nearby SNPs to minimize confounding effects. Additionally, the chosen
232 SNPs had a minor allele frequency (MAF) > 0.01 to ensure adequate
233 statistical power. After this initial filtering, we further ensured that the
234 variations were reflective of the effects of exposure on outcome; any
235 SNPs with F-statistics < 10 or failure to harmonize, including those

236 harboring incompatible alleles or palindromic characteristics with
237 intermediate allele frequencies, were excluded. Correct inference
238 direction from exposure to outcome was identified using the Steiger
239 filtering approach, to lessen the influence of reverse association. Finally,
240 we used the NHGRI-EBI Catalog (<https://www.ebi.ac.uk/gwas/>) to
241 retrieve these SNPs and excluded SNPs related to confounding factors
242 and outcomes (education, living habits, smoking, diet) [97]. Figure 1
243 summarizes this selection process.

244

245 4. Statistical analyses

246 We used R version 4.2.0 for all statistical analyses. We employed various
247 statistical methodologies to evaluate the causal influence of GM on
248 chronic pain phenotypes. Commonly used approaches included the
249 multiplicative random effects–inverse-variance weighted (MRE-IVW)
250 [56], weighted mode (WM) [26], weighted median (WME) [8], and
251 MR-Egger regression [7]. Additionally, we incorporated more recent
252 methods like contamination mixture (ConMix) [14], MR-robust adjusted
253 profile score (MR-RAPS)[96], debiased inverse-variance weighted
254 (dIVW) method [94], and cML-MA [93] to enhance the robustness of our
255 findings. False discovery rate (FDR) correction was applied to strengthen
256 the statistical power of the results. Given the potential bias in IVW
257 estimation when pleiotropic IVs were utilized [13], several sensitivity

258 analyses were conducted to address pleiotropy in the causal estimates,
259 including Cochran's Q statistic for heterogeneity ($P > 0.05$) [9], MR-Egger
260 regression for horizontal pleiotropy [7] and its intercept term ($P > 0.05$),
261 MR-PRESSO [84] for further evaluation of horizontal pleiotropy,
262 leave-one-out analysis to evaluate the influence of individual SNPs on the
263 observed associations, and power calculations using a non-centrality
264 parameter-based approach [11] and publicly available mRnd web tool
265 (<http://cnsgenomics.com/shiny/mRnd/>). Any results with evidence of
266 confounding by pleiotropy were excluded (Online Methods). We also
267 limited our analysis to pairs of variables supported by at least three
268 genetic variants.

269 We used meta-analysis to identify the positive GM, which were then
270 subjected to mediation analysis. To verify whether the screened positive
271 GM and pain phenotype share the same causal variation in a given region
272 (50 kb above and below each SNP), we employed genetic colocalization
273 analysis (coloc). Furthermore, Bayesian weighted MR (BWMR) was
274 implemented to strengthen the evidence for a causal relationship between
275 the identified positive GM and pain phenotypes [95]. We also examined
276 the impact of these potential positive GM on specific brain regions within
277 the cerebral cortex.

278 To assess the potential mediating role of the intermediary effect (IE) on
279 the relationship between the exposure (a) and the outcome (c'), we

280 conducted a mediation analysis using an interactive mediation framework
281 and Sobel tests (<http://quantpsy.org/sobel/sobel.htm>) (Figure 1(b-2)). The
282 IVW method was employed to estimate the causal effects, including IE
283 ($a*b$), direct effect (DE; $c' - (a*b)$), and total effect (TE; c'). Statistical
284 significance was determined by a two-sided P-value threshold of 0.05.
285 We employed FDR correction to account for multiple comparisons when
286 evaluating statistical significance. Associations with an FDR of <0.05
287 were considered statistically significant. However, we expanded the
288 p-value of the meta-analysis to 0.1 when no p-value was less than 0.05.
289 We acknowledge the exploratory nature of this study and report both raw
290 P and FDR values.

291

292 5 Results

293 5.1 Preliminary results of MR: GM on MCP and eight pain phenotypes

294 5.1.1 GM on MCP

295 We observed that 4 taxa (2 orders and 2 families) were related to MCP in
296 Data 1, 8 taxa (2 genera, 2 OTU97, 2 OTU99, and 2 TestASV) were
297 related to MCP in Data 2, 11 taxa (1 phylum, 1 class, 1 order, 2 families,
298 2 genera, and 4 species) were related to MCP in Data 3, and 18 taxa (1
299 class, 2 orders, 1 family, 7 genera, and 7 unclassified) were related to
300 MCP in Data 4. (see Supplementary 1)

301

302 5.1.2 GM on Headache

303 We observed that 7 taxa (1 phylum, 1 class, 1 order, 2 families, and 2
304 genera) were related to headache in Data 1, 9 taxa (1 class, 1 order, 1
305 family, 1 OTU97, 1 OTU99, and 4 TestASV) were related to headache in
306 Data 2, 7 taxa (1 order, 1 family, 2 genera, and 3 species) were related to
307 headache in Data 3, and 17 taxa (1 order, 2 families, 6 genera, 2 species,
308 and 6 unclassified) were related to headache in Data 4.(see
309 Supplementary 2)

310

311 5.1.3 GM on Facial Pain

312 We observed that 6 taxa (1 order, 2 families, and 3 genera) were related to
313 facial pain in Data 1, 9 taxa (1 genus, 4 OTU97, 3 OTU99, and 1
314 TestASV) were related to facial pain in Data 2, 5 taxa (1 family, 1 genus,
315 and 3 species) were related to facial pain in Data 3, and 22 taxa (2 phyla,
316 1 order, 2 families, 9 genera, 2 species, and 7 unclassified) were related to
317 facial pain in Data 4. (see Supplementary 3)

318

319 5.1.4 GM on Neck/Shoulder Pain

320 We observed that 4 taxa (1 phylum, 2 families, and 1 genus) were related
321 to neck/shoulder pain in Data 1, 5 taxa (1 class, 1 family, 1 OTU97, 1
322 OTU99, and 1 TestASV) were related to neck/shoulder pain in Data 2, 5
323 taxa (1 class, 1 order, 1 family, 1 genus, and 1 species) were related to

324 neck/shoulder pain in Data 3, and 20 taxa (1 family, 10 genera, 2 species,
325 and 7 unclassified) were related to neck/shoulder pain in Data 4.(see
326 Supplementary 4)

327

328 5.1.5 GM on Abdominal Pain

329 We observed that 8 taxa (1 class, 2 orders, 2 families, and 3 genera) were
330 related to abdominal pain in Data 1, 8 taxa (1 class, 1 genus, 3 OTU97, 2
331 OTU99, and 1 TestASV) were related to abdominal pain in Data 2, 3 taxa
332 (3 species) were related to abdominal pain in Data 3, and 19 taxa (2
333 orders, 1 family, 9 genera, 3 species, and 4 unclassified) were related to
334 abdominal pain in Data 4. (see Supplementary 5)

335

336 5.1.6 GM on Back Pain

337 We observed that 5 taxa (1 phylum, 1 class, 1 order, and 2 genera) were
338 related to back pain in Data 1, 6 taxa (1 family, 1 genus, 2 OTU97, and 2
339 OTU99) were related to back pain in Data 2, 3 taxa (1 order, 1 family, and
340 1 species) were related to back pain in Data 3, and 16 taxa (2 classes, 2
341 families, 7 genera, 1 species, and 4 unclassified) were related to back pain
342 in Data 4. (see Supplementary 6)

343

344 5.1.7 GM on Hip Pain

345 We observed that 7 taxa (1 family and 6 genera) were related to hip pain

346 in Data 1, 8 taxa (3 OTU97, 3 OTU99, and 2 TestASV) were related to
347 hip pain in Data 2, 8 taxa (1 family, 4 genera, and 3 species) were related
348 to hip pain in Data 3, and 17 taxa (2 orders, 2 families, 8 genera, and 5
349 unclassified) were related to hip pain in Data 4. (see Supplementary 7)

350

351 5.1.8 GM on Knee Pain

352 We observed that 11 taxa (2 phyla, 2 classes, 3 orders, and 4 genera) were
353 related to knee pain in Data 1, 3 taxa (3 OTU99) were related to knee
354 pain in Data 2, 5 taxa (1 family and 4 genera) were related to knee pain in
355 Data 3, and 21 taxa (2 orders, 5 families, 9 genera, and 5 unclassified)
356 were related to knee pain in Data 4. (see Supplementary 8)

357

358 5.1.9 GM on Pain All Over the Body

359 We observed that 5 taxa (5 genera) were related to pain all over the body
360 in Data 1, 11 taxa (1 class, 1 order, 1 family, 2 OTU97, 5 OTU99, and 1
361 TestASV) were related to pain all over the body in Data 2, 10 taxa (1
362 class, 2 orders, 3 families, 2 genera, and 2 species) were related to pain all
363 over the body in Data 3, and 21 taxa (11 genera, 3 species, and 7
364 unclassified) were related to pain all over the body in Data 4. (see
365 Supplementary 9)

366 After adjusting the p-values by FDR, Genus *Odoribacter* was still
367 significantly associated with neck/shoulder pain ($P_{IVW} = 1.203 \times 10^{-4}$,

368 $P_{\text{FDR}} = 0.048$).

369

370 5.2 Results of meta-analysis: GM on MCP and eight pain phenotypes

371 In the second step, we conducted a meta-analysis based on the

372 preliminary results from Section 5.1 in this exploratory study (see Table 2,

373 Figure 2 and 3).

374 **MCP:** The abundance of Genus *Adlercreutzia* ($P_{\text{IVW}} = 3.71\text{E-}02$, $P_{\text{Meta}} =$

375 $2.24\text{E-}02$) was positively associated with MCP, while that of Phylum

376 *Verrucomicrobia* ($P_{\text{IVW}} = 1.90\text{E-}02$, $P_{\text{Meta}} = 1.12\text{E-}02$) was negatively

377 associated with MCP.

378 **Headache:** The abundance of Phylum *Verrucomicrobia* ($P_{\text{IVW}} = 2.02\text{E-}02$,

379 $P_{\text{Meta}} = 2.32\text{E-}02$) was negatively associated with headache.

380 **Facial Pain:** The abundances of Genus *Alistipes* ($P_{\text{IVW}} = 1.17\text{E-}02$, $P_{\text{Meta}} =$

381 $4.68\text{E-}02$) and Genus *Bifidobacterium* ($P_{\text{IVW}} = 1.43\text{E-}02$, $P_{\text{Meta}} = 4.48\text{E-}02$)

382 were positively associated with facial pain.

383 **Neck/Shoulder Pain:** The abundances of Class *Alphaproteobacteria*

384 ($P_{\text{IVW}} = 4.92\text{E-}02$, $P_{\text{Meta}} = 1.17\text{E-}02$) and Genus *Odoribacter* ($P_{\text{IVW}} =$

385 $1.20\text{E-}04$, $P_{\text{Meta}} = 5.54\text{E-}05$) were negatively associated with

386 neck/shoulder pain.

387 **Abdominal Pain:** The abundances of Class *Gammaproteobacteria* (P_{IVW}

388 $= 3.10\text{E-}02$, $P_{\text{Meta}} = 1.95\text{E-}02$) and Species *Eubacterium eligens* ($P_{\text{IVW}} =$

389 $3.72\text{E-}02$, $P_{\text{Meta}} = 1.18\text{E-}02$) were positively associated with abdominal

390 pain, while that of Genus *Alistipes* ($P_{IVW} = 3.46E-02$, $P_{Meta} = 3.71E-02$)
391 was negatively associated with abdominal pain.

392 **Back Pain:** The abundance of Order *Bifidobacteriales* ($P_{IVW} = 3.99E-02$,
393 $P_{Meta} = 4.83E-02$) was positively associated with back pain.

394 **Pain All Over the Body:** The abundance of Genus *Ruminococcus2* (P_{IVW}
395 $= 1.46E-03$, $P_{Meta} = 2.81E-03$) was positively associated with pain all over
396 the body, while Genus *Desulfovibrio* ($P_{IVW} = 7.01E-03$, $P_{Meta} = 1.49E-02$)
397 was negatively associated with pain all over the body.

398 In this exploratory study, we expanded the P-value threshold for the
399 meta-analysis to 0.1. The following associations were observed:

400 **Back Pain:** The abundance of Family *Prevotellaceae* ($P_{IVW} = 1.15E-02$,
401 $P_{Meta} = 5.20E-02$) was negatively associated with back pain.

402 **Hip Pain:** The abundance of Genus *Subdoligranulum* ($P_{IVW} = 4.09E-02$,
403 $P_{Meta} = 8.41E-02$) was negatively associated with hip pain.

404 **Knee Pain:** The abundance of Genus *Dialister* ($P_{IVW} = 3.94E-02$, $P_{Meta} =$
405 $7.69E-02$) was negatively associated with knee pain.

406

407 5.3 Results of BWMR and coloc analysis: GM on MCP and eight pain
408 phenotypes

409 To further strengthen the causal inference between the identified GM
410 features and chronic pain phenotypes, we employed both BWMR and
411 colocalization analyses. 13 positive GMs were still causally related to

412 MCP and eight pain phenotypes in BWMR, except for Class
413 *Alphaproteobacteria* on neck/shoulder pain ($P_{\text{BWMR}} = 5.73\text{E-}02$) (see
414 Table 2).

415 The PP.H4.abf values of the 13 positive GMs ranged from 0.001691934
416 to 0.055804256. No data were found in the target region for the
417 remaining three positive GMs. Colocalization analysis findings further
418 strengthened the causal relationship between positive GM and MCP and
419 eight pain phenotypes (See Table 2 and 3, Figure 3 and 4).

420

421 5.4 Results of MR: GM on BID phenotypes and human cerebral cortex

422 5.4.1 GM on BID Phenotypes (see Supplementary 10)

423 5.4.1.1 Data 1

424 **Genus *Desulfovibrio***: Its abundance was positively associated with the
425 rostral middle frontal area in the right hemisphere ($P_{\text{IVW}} = 3.79\text{E-}02$) and
426 negatively associated with rfMRI connectivity (ICA100 edge 1064) (P_{IVW}
427 $= 3.47\text{E-}02$), for which detailed information was not found.

428 **Genus *Ruminococcus2***: Its abundance was positively associated with the
429 putamen volume in the right hemisphere ($P_{\text{IVW}} = 2.94\text{E-}02$), insula
430 volume in the left ($P_{\text{IVW}} = 3.19\text{E-}02$) and right hemispheres ($P_{\text{IVW}} =$
431 $4.72\text{E-}02$), and G+S-occipital-inf area in the right hemisphere ($P_{\text{IVW}} =$
432 $2.17\text{E-}02$).

433 5.4.1.2 Data 2

434 **Class *Gammaproteobacteria***: Its abundance was positively associated
435 with the medial geniculate nucleus (MGN) volume in the right
436 hemisphere ($P_{IVW} = 1.03E-02$) and negatively associated with the
437 S-intrapariet+P-trans volume in the left hemisphere ($P_{IVW} = 4.87E-02$), as
438 well as positively associated with connectivity ICA100 edge 819 ($P_{IVW} =$
439 $4.90E-02$) and negatively associated with connectivity ICA100 edge 1063
440 ($P_{IVW} = 2.89E-02$), for which detailed information was not found.

441 **Family *Prevotellaceae***: Its abundance was positively associated with the
442 weighted mean L1 in trace left posterior thalamic radiation ($P_{IVW} =$
443 $1.67E-02$).

444 5.4.1.3 Data 3

445 **Genus *Odoribacter***: Its abundance was positively associated with mean
446 OD in the Fornix crescent+stria terminalis (left) ($P_{IVW} = 1.49E-04$).

447 **Genus *Subdoligranulum***: Its abundance was positively associated with
448 the weighted mean L2 in trace right cingulate gyrus part cingulum ($P_{IVW} =$
449 $3.00E-02$).

450 **Genus *Dialister***: Its abundance was negatively associated with the mean
451 TH of G-pariet-inf-Supramar in the left hemisphere ($P_{IVW} = 4.79E-02$).

452 **Order *Bifidobacteriales***: Its abundance was negatively associated with
453 the hippocampal tail volume in the right hemisphere ($P_{IVW} = 3.11E-03$).

454 5.4.1.4 Data 4

455 **Genus *Alistipes***: Its abundance was positively associated with the

456 weighted mean diffusion tensor mode (MO) in the left superior
457 longitudinal fasciculus ($P_{IVW} = 3.01E-02$) and mean OD in the Fornix
458 crescent+stria terminalis (right) on fractional anisotropy (FA) skeleton
459 ($P_{IVW} = 4.94E-02$) and negatively associated with the mean TH of the
460 posterior cingulate in the left hemisphere ($P_{IVW} = 1.49E-02$), mean MO in
461 the inferior cerebellar peduncle (left) on FA skeleton ($P_{IVW} = 4.72E-02$),
462 corticoamygdaloid transition volume in the right hemisphere ($P_{IVW} =$
463 $1.12E-03$), and medial orbitofrontal cortex volume in the left hemisphere
464 ($P_{IVW} = 4.02E-03$).

465 **Genus *Bifidobacterium***: Its abundance was positively associated with
466 connectivity (ICA100 edge 405) ($P_{IVW} = 2.31E-02$), for which detailed
467 information was not found, and negatively associated with the mean TH
468 of the parstriangularis ($P_{IVW} = 1.69E-03$) and S-circular-insula-sup (P_{IVW}
469 $= 4.09E-03$) in the left hemisphere; mean TH of the G-insular-short in the
470 right hemisphere ($P_{IVW} = 3.36E-03$); mean OD in the body of the corpus
471 callosum ($P_{IVW} = 3.06E-02$) and Fornix crescent+stria terminalis (right)
472 on the FA skeleton ($P_{IVW} = 4.47E-02$); HATA volume ($P_{IVW} = 5.89E-03$)
473 and area of isthmus cingulate ($P_{IVW} = 2.66E-03$) in the left hemisphere;
474 G-front-middle volume ($P_{IVW} = 4.58E-02$), S-circular-insula-inf volume
475 ($P_{IVW} = 4.85E-02$), and area of superior temporal ($P_{IVW} = 2.95E-02$) in the
476 right hemisphere; and rfMRI amplitudes (ICA100 node 27) ($P_{IVW} =$
477 $5.89E-03$), for which detailed information was not found.

478

479 5.4.2 GM on the Human Cerebral Cortex (see Supplementary 11)

480 5.4.2.1 Data 1

481 **Genus *Desulfovibrio***: Its abundance was positively associated with mean
482 SA of the paracentral ($P_{IVW} = 4.57E-02$) and mean TH of the frontal pole
483 ($P_{IVW} = 2.60E-02$) and negatively associated with mean SA of the
484 superior parietal ($P_{IVW} = 3.48E-02$).

485 **Genus *Ruminococcus2***: Its abundance was positively associated with
486 mean SA of the bankssts ($P_{IVW} = 3.83E-02$) and fusiform ($P_{IVW} =$
487 $1.61E-02$).

488 **Phylum *Verrucomicrobia***: Its abundance was negatively associated with
489 mean SA of the lateral orbitofrontal ($P_{IVW} = 3.04E-02$).

490 5.4.2.2 Data 2

491 **Class *Gammaproteobacteria***: Its abundance was positively associated
492 with mean SA of the bankssts ($P_{IVW} = 4.80E-02$), paracentral ($P_{IVW} =$
493 $4.47E-02$), posterior cingulate ($P_{IVW} = 1.97E-03$), and precentral ($P_{IVW} =$
494 $2.27E-02$) and negatively associated with the mean TH of the isthmus
495 cingulate ($P_{IVW} = 4.04E-02$).

496 **Family *Prevotellaceae***: Its abundance was negatively associated with
497 mean TH of the inferior parietal ($P_{IVW} = 2.33E-03$).

498 5.4.2.3 Data 3

499 **Genus *Odoribacter***: Its abundance was positively associated with the

500 mean TH of lateral occipital ($P_{IVW} = 3.22E-02$) and negatively associated
501 with the mean TH of superior frontal ($P_{IVW} = 3.46E-02$).

502 **Genus *Subdoligranulum***: Its abundance was negatively associated with
503 the mean TH of the rostral middle frontal cortex ($P_{IVW} = 4.19E-02$).

504 **Genus *Dialister***: Its abundance was positively associated with the mean
505 TH of middle temporal ($P_{IVW} = 4.16E-02$) and negatively associated with
506 the mean SA of inferior parietal ($P_{IVW} = 4.91E-02$) and precentral ($P_{IVW} =$
507 $4.46E-02$).

508 **Species *E. eligens***: Its abundance was positively associated with the
509 mean SA of posterior cingulate ($P_{IVW} = 3.02E-02$).

510 **Phylum *Verrucomicrobia***: Its abundance was positively associated with
511 global full SA ($P_{IVW} = 4.83E-02$) and the mean SA of caudal middle
512 frontal ($P_{IVW} = 3.77E-02$), insula ($P_{IVW} = 8.68E-03$), superior temporal
513 ($P_{IVW} = 3.40E-02$), and TH of postcentral ($P_{IVW} = 2.87E-02$) and rostral
514 anterior cingulate ($P_{IVW} = 2.91E-02$) and negatively associated with the
515 mean SA of pericalcarine ($P_{IVW} = 3.32E-02$).

516 **Genus *Adlercreutzia***: Its abundance was positively associated with the
517 mean SA of lateral occipital ($P_{IVW} = 3.39E-02$).

518 5.4.2.4 Data 4

519 **Genus *Alistipes***: Its abundance was positively associated with the mean
520 SA of lateral occipital ($P_{IVW} = 2.61E-02$) and negatively associated with
521 the mean SA of fusiform ($P_{IVW} = 1.66E-03$) and postcentral ($P_{IVW} =$

522 4.62E-02).

523 **Genus *Bifidobacterium***: Its abundance was positively associated with the
524 mean TH of posterior cingulate ($P_{IVW} = 4.32E-02$) and negatively
525 associated with the mean SA of supramarginal ($P_{IVW} = 1.83E-03$) and
526 transverse temporal ($P_{IVW} = 7.67E-03$).

527 5.4.2 GM on 83 Brain Regions (see Supplementary 12)

528 **Class *Gammaproteobacteria***: Its abundance was negatively associated
529 with the left superior parietal volume ($P_{IVW} = 3.07E-02$).

530 **Genus *Bifidobacterium***: Its abundance was negatively associated with
531 the right caudal middle frontal volume ($P_{IVW} = 1.97E-02$). No causal
532 effects were observed for the other 13 genetic predispositions on 83 brain
533 regions because their P_{IVW} s were >0.05 .

534

535 5.5 Results of mediation analysis

536 5.5.1 GM on MCP and eight pain phenotypes (See Table 4, Fig 5,
537 Supplementary 13)

538 Finally, we conducted a mediation analysis to explore the primary
539 mediating GBA model of MCP and eight pain phenotypes based on
540 Sections 5.2 and 5.3. Our findings indicate that the causal effect between
541 Genus *Odoribacter* and neck/shoulder pain could be mediated by mean
542 OD in Fornix cres + Stria terminalis (left) (Table 4). For Genus
543 *Odoribacter* - mean OD in Fornix cres+Stria terminalis (left) -

544 neck/shoulder pain, TE = -0.020, IE = -0.003, DE = -0.017 (P = 0.027),
545 IE_div_TE = 0.140 (0.013-0.267) (see Figure 5).

546

547 6. Discussion

548 6.1. GM and pain phenotypes

549 This study is the first to analyze the causal association of GM with MCP
550 and eight pain phenotypes by MR, incorporating human brain structures.

551 Furthermore, we were able to establish a GBA model linking Genus
552 *Odoribacter* to neck/shoulder pain. We identified 13 potential relevant

553 GM. Importantly, different pain phenotypes were causally associated with
554 specific GM. Seven positive and eight negative causal associations were

555 found, among which Genus *Odoribacter* as a protective GM for
556 neck/shoulder pain needs to be emphasized.

557 Previous MR studies did not identify GM overlapping with those within
558 our study, except for Family *Prevotellaceae*. This discrepancy may stem

559 from previous studies predominantly focusing on specific pain-related
560 diseases as outcomes, while our study examined pain phenotypes.

561 Notably, our study suggests that Family *Prevotellaceae* provides
562 protection against back pain, whereas previous MR studies reported it

563 increases the risk of low back pain [23,78]. This difference could be
564 attributed to variations in study outcomes and methodologies; previous

565 studies often utilized single GM databases, whereas we incorporated four

566 different GM databases and conducted a meta-analysis.

567 Meanwhile, our results suggest Phylum *Verrucomicrobia* and Genus
568 *Dialister* are protective factors for CP, while Genus *Adlercreutzia* is risk
569 factor, consistent with previous observational studies [18,23,30,40-41,85].
570 Despite variations in associated pain sites, this reinforces the potential
571 role of these GMs in pain pathogenesis. Conversely, previous
572 observational studies involving Genus *Desulfovibrio*, Genus
573 *Subdoligranulum*, and Genus *Odoribacter* have yielded inconsistent
574 results [17,23,86-88]. Our study's findings may be more compelling due
575 to its ability to establish causation, which observational studies cannot
576 confirm definitively as they often have small sample sizes.

577 Interestingly, despite its probiotic properties in inhibiting pain behaviors
578 [55], Genus *Bifidobacterium* was found to increase the risk of facial pain
579 in our study, aligning with previous inconsistent findings [23,54,59].
580 Similarly, Genus *Adlercreutzia*, recognized for its health benefits [10],
581 has been associated with back pain [18] and identified as a risk factor for
582 MCP in our study. A recent attempt to use *Bifidobacterium* in treating
583 neuropathic pain was unsuccessful [28], suggesting that the effects of
584 symbionts may be complicated through interactions with pathobionts that
585 are associated with pain conditions. The role of GM in CP is complex,
586 possibly involving differential effects within microbial networks [10].
587 Future research may benefit from constructing gut microbial networks

588 based on key GMs to elucidate CP mechanisms.

589

590 6.2. The gut-brain axis

591 Pain is a dynamic interplay between sensory, emotional, and cognitive

592 factors [48] processed within the pain matrix-a network of interconnected

593 brain regions [15], especially CP. Emerging research suggests a potential

594 influence of GM in modulating pain perception [45]. Since changes in

595 brain structure can significantly affect its function [57], we investigated

596 the potential connection between GM and brain regions involved in pain

597 processing using brain imaging data. In general, except for Family

598 *Prevotellaceae*, Genus *Subdoligranulum*, Order *Bifidobacteriales*, and

599 Species *E. eligens*, the remaining positive GMs have been potentially

600 causally linked to the brain regions primarily involved in sensory,

601 emotional, and cognitive functions, which may help us partly understand

602 how GM affect CP.

603 Firstly, we found that multiple positive GM could affect the area of

604 pain-related cerebral cortex. In our study, the abundance of Phylum

605 *Verrucomicrobia*, a protective factor against MCP and headache, was not

606 only positively associated with the entire cortical area, but also positively

607 correlated with the area of caudal middle frontal and insula. This finding

608 extends the results of a recent study on CP utilizing the UK Biobank data

609 [5]. Other studies suggest that the anterior insula plays a more important

610 role in anticipating pain and its emotional features, while the posterior
611 insula is more active during the physical sensations of pain [55, 58, 68].
612 The observed protective effect of Phylum *Verrucomicrobia* on these
613 regions aligns with the possibility that these bacteria might help in
614 maintaining normal brain function related to pain perception. This finding
615 offers a potential target for future research on chronic pain management
616 strategies.

617 Furthermore, our study revealed that Genus *Desulfovibrio* was not only
618 positively correlated with the area of rostral middle frontal cortex which
619 are crucial for emotional and cognitive processing, but also positively
620 correlated with the paracentral area and negatively with the
621 superiorparietal area belonging sensorimotor cortices. As a protective
622 factor for chronic multisite pain, the interaction between these affected
623 brain areas deserves further exploration.

624 Secondly, we found that multiple positive GM could affect the thickness
625 and volume of pain-related cerebral cortex. CP patients often show
626 reduced gray matter volume in several brain regions, including areas
627 involved in processing pain, managing emotions, and controlling
628 movement [3-4,6,20,32,35,46-47,51-52,64,70-71,73,91]. Certain GM
629 may have either positive or negative effects on the volume of these brain
630 regions. For example, Phylum *Verrucomicrobia* abundance was
631 associated with thicker gray matter in the rostral-anterior-cingulate and

632 postcentral regions, further supporting its protective role against CP.
633 Additionally, multiple GM were found to significantly influence one
634 brain region, such as the frontal lobe. This finding suggests that the
635 observed decrease in gray matter volume in CP patients may result from
636 the combined effects of multiple GM.

637 Thirdly, this study reveals that GM may influence chronic pain by
638 affecting the integrity and direction of axonal fiber dispersion in white
639 matter. CP patients often exhibit changes in the microstructure of white
640 matter, like superior longitudinal fasciculus, corpus callosum, and
641 cingulum bundle, which play crucial roles in pain severity, resilience and
642 emotional response to pain [52,69,81,89]. Our results indicate that certain
643 positive GM can positively (Genus *Subdoligranulum*-cingulum bundle
644 (rh)) or negatively (Genus *Bifidobacterium*-corpus callosum) influence
645 white matter in specific locations. Observational studies have also linked
646 reduced white matter integrity in the splenium of the corpus callosum to
647 chronic low back pain disability [12]. Our study found that Family
648 *Prevotellaceae* abundance positively affected posterior-thalamic-radiation
649 (lh), supporting its role as a protective factor against back pain.

650 Morphological changes in the limbic system are closely linked to
651 persistent pain. Particularly, the Fornix cres+Stria terminalis region needs
652 to be emphasized, which is positively affected by Genus *Odoribacter* and
653 Genus *Alistipes* and negative affected by Genus *Bifidobacterium*. Notably,

654 our findings suggest that the causal relationship between Genus
655 *Odoribacter* abundance and neck/shoulder pain may be mediated by
656 mean OD in the Fornix cres+Stria terminalis (left).

657 The fornix, crucial for normal cognitive function [80], has also been
658 associated with pain abnormalities [43]. Similarly, the stria terminalis is
659 integral to the limbic system, connecting the amygdala to the
660 hypothalamus. Although the fornix and stria terminalis are not directly
661 connected, they create an indirect anatomical pathway between the
662 hippocampus and the amygdala. Through shared connections to structures
663 like the hypothalamus and septal nuclei, these regions can influence each
664 other, forming a corticolimbic system critical in the initiation, persistence,
665 and amplification of chronic pain states [1,83], and influencing the
666 transition from acute to chronic pain [91]. Continued activation of
667 corticolimbic circuits results in functional and anatomical changes in the
668 cortex, contributing to prolonged pain states [91].

669 Our study identified new avenues for investigating the GBA in chronic
670 pain and pain phenotypes. The Fornix cres+Stria terminalis is highlighted
671 as a new factor in the GBA and a novel key area for CP (Genus
672 *Odoribacter* to neck/shoulder pain). Targeted therapies focusing on these
673 areas may offer innovative approaches to pain management and
674 treatment.

675 There are some contradictions in the results: Genus *Alistipes* appears to

676 exert contrasting influences in abdominal and facial pain. Class
677 *Gammaproteobacteria* abundance was positively correlated with the
678 paracentral and precentral areas but acted as a risk factor for abdominal
679 pain, and Genus *Dialister* abundance was negatively associated with the
680 precentral area but served as a protective factor for knee pain. Various
681 internal brain networks and regulatory systems collaboratively contribute
682 to the experience and persistence of chronic pain [16,19,46]. Future
683 research using multimodal fMRI to investigate how GM influences these
684 brain network changes may provide insights into these findings.

685

686 Limitations and strengths

687 Our study has some advantages. First, we employed a comprehensive set
688 of sensitivity analyses, including meta-analyses and colocalization
689 analyses. These analyses provide strong evidence that our findings are
690 robust. Second, we addressed potential biases by applying methods like
691 MR-Egger and MR-PRESSO to assess pleiotropy (where a genetic
692 variant influences multiple traits) and identify outliers. Those steps
693 helped to ensure the reliability of our MR results. Finally, the analysis
694 utilized powerful IVs (F-statistics > 10), minimizing the influence of
695 weak instruments that could bias the MR results.

696 However, our study also has certain limitations. Firstly, the data
697 originated from participants of European ancestry. Secondly, we did not

698 conduct reverse MR analyses or MR analyses directly analyzing the
699 relationship between pain phenotypes and brain structure, which will be
700 explored in future studies. Thirdly, to ensure a sufficient number of IVs
701 for GM, we employed a significance threshold of $P < 1 \times 10^{-5}$, which is less
702 stringent than the genome-wide significance level ($P < 5 \times 10^{-8}$).

703

704 Conclusions

705 Among European ancestry, we identified 13 GM that were causally
706 related to chronic pain; 8 GM decreased risk towards MCP and pain
707 phenotypes, and 7 GM increased risk. Core GM may influence CP by
708 affecting complex brain networks associated with emotional, cognitive,
709 and motor functions. Specifically, we constructed a basic GBA model for
710 neck/shoulder pain with Genus *Odoribacter* - Fornix cres+Stria
711 terminalis (left) interactions playing a key role in neck/shoulder pain. Our
712 study contributes to novel insights into the relationships between specific
713 GM and pain phenotypes, supporting that GBA play a key role in the
714 pathogenesis of CP. Consequently, the GBA is a new drug target to treat
715 CP through neuroregulatory therapies and targeted treatments with
716 protective symbionts.

717

718 Reference

719 [1] Apkarian A.V., Baliki M.N., Geha P.Y.,2009. Towards a theory of chronic pain.Prog

- 720 Neurobiol 87(2):81-97. doi: 10.1016/j.pneurobio.2008.09.018.
- 721 [2] Apkarian A.V., Bushnell M.C., Treede R.D., Zubieta J.K., 2005. Human brain mechanisms
722 of pain perception and regulation in health and disease. Eur J Pain 9(4):463-84. doi:
723 10.1016/j.ejpain.2004.11.001.
- 724 [3] Apkarian A.V., Sosa Y., Sonty S., Levy R.M., Harden R.N., Parrish T.B., Gitelman
725 D.R.,2004.Chronic Back Pain Is Associated with Decreased Prefrontal and Thalamic Gray
726 Matter Density. J Neurosci 24(46):10410-5. doi: 10.1523/JNEUROSCI.2541-04.2004.
- 727 [4] Bhatt R.R., Gupta A., Mayer E.A., Zeltzer L.K., 2020. Chronic pain in children: structural
728 and resting-state functional brain imaging within a developmental perspective. Pediatr Res
729 88(6):840-849. doi: 10.1038/s41390-019-0689-9. Epub 2019 Dec 2.
- 730 [5] Bhatt R.R., Haddad E., Zhu A.H., Thompson P.M., Gupta A., Mayer E.A., Jahanshad N.,
731 2024. Mapping Brain Structure Variability in Chronic Pain: The Role of Widespreadness and
732 Pain Type and its Mediating Relationship with Suicide Attempt. Biol Psychiatry
733 95(5):473-481. doi: 10.1016/j.biopsych.2023.07.016.
- 734 [6] Borsook D., Erpelding N., Becerra L., 2013. Losses and gains: chronic pain and altered
735 brain morphology. Expert Rev Neurother 13(11):1221-34. doi:
736 10.1586/14737175.2013.846218.
- 737 [7] Bowden J., Davey Smith G., Burgess S., 2015. Mendelian randomization with invalid
738 instruments: effect estimation and bias detection through Egger regression. Int. J. Epidemiol.
739 44, 512–525.
- 740 [8] Bowden J., Davey Smith G., Haycock P.C., Burgess S., 2016. Consistent estimation in
741 Mendelian randomization with some invalid instruments using a weighted median estimator.

- 742 Genet. Epidemiol. 40, 304–314.
- 743 [9] Bowden J., Fabiola Del Greco M., Minelli G., Smith G.D., Sheehan N., Thompson J.,
744 2017. A framework for the investigation of pleiotropy in two-sample summary data
745 Mendelian randomization. Stat. Med. 36, 1783–1802.
- 746 [10] Brandon-Mong G.J., Shaw G.T.W., Chen W.H., Chen C.C., Wang D., 2020. A network
747 approach to investigating the key microbes and stability of gut microbial communities in a
748 mouse neuropathic pain model. BMC Microbiol 20(1):295. doi: 10.1186/s12866-020-01981-7.
- 749 [11] Brion M.J., Shakhbazov K., Visscher P.M., 2013. Calculating statistical power in
750 Mendelian randomization studies. Int. J. Epidemiol. 42, 1497–1501.
- 751 [12] Buckalew N., Haut M.W., Aizenstein H., Rosano C., Edelman K.D., Perera S., Marrow
752 L., Tadic S., Venkatraman V., Weiner D., 2013. White matter hyperintensity burden and
753 disability in older adults: is chronic pain a contributor? PM R 5(6):471-80; quiz 480. doi:
754 10.1016/j.pmrj.2013.03.004.
- 755 [13] Burgess S., Butterworth A., Thompson S.G., 2013. Mendelian randomization analysis
756 with multiple genetic variants using summarized data. Genet. Epidemiol. 37, 658–665.
- 757 [14] Burgess S., Foley C.N., Allara E., Staley J.R., Howson J.M.M., 2020. A robust and
758 efficient method for Mendelian randomization with hundreds of genetic variants. Nat
759 Commun 11(1):376. doi: 10.1038/s41467-019-14156-4.
- 760 [15] Bushnell M.C., Ceko M., Low L.A., 2013. Cognitive and emotional control of pain and
761 its disruption in chronic pain. Nat Rev Neurosci 14(7):502-511. doi: 10.1038/nrn3516.
- 762 [16] Canavero S., Bonicalzi V., 2015. Pain myths and the genesis of central pain. Pain Med
763 16(2):240-248. doi: 10.1111/pme.12509.

- 764 [17] Chriswell M.E., Lefferts A.R., Clay M.R., Hsu A.R., Seifert J., Feser M.L., Rims C.,
765 Bloom M.S., Bemis E.A., Liu S., Maerz M.D., Frank D.N., Demoruelle M.K., Deane K.D.,
766 James E.A., Buckner J.H., Robinson W.H., Holers V.M., Kuhn K.A., 2022. Clonal IgA and
767 IgG autoantibodies from individuals at risk for rheumatoid arthritis identify an arthritogenic
768 strain of Subdoligranulum. *Sci Transl Med* 14(668):eabn5166. doi:
769 10.1126/scitranslmed.abn5166.
- 770 [18] Dekker Nitert M., Mousa A., Barrett H. L., Naderpoor N., de Courten B., 2020. Altered
771 gut microbiota composition is associated with Back pain in overweight and obese individuals.
772 *Front. Endocrinol.* 11:605. doi: 10.3389/fendo.2020.00605.
- 773 [19] Fitzcharles M.A., Cohen S.P., Clauw D.J., Littlejohn G., Usui C., Häuser W., 2021.
774 Nociceptive pain: towards an understanding of prevalent pain conditions. *Lancet*
775 397(10289):2098-2110. doi: 10.1016/S0140-6736(21)00392-5.
- 776 [20] Fritz J.H., Wittfeld K., Hegenscheid K., Schmidt C.O., Langner S., Lotze
777 M., 2016. Chronic Back Pain Is Associated With Decreased Prefrontal and Anterior Insular
778 Gray Matter: Results From a Population-Based Cohort Study. *J Pain* 17(1):111-8. doi:
779 10.1016/j.jpain.2015.10.003.
- 780 [21] Fürtjes A.E., Arathimos R., Coleman J.R.I., Cole J.H., Cox S.R., Deary I.J., de la Fuente
781 J., Madole J.W., Tucker-Drob E.M., Ritchie S.J., 2023. General dimensions of human brain
782 morphometry inferred from genome-wide association data. *Hum Brain Mapp* 44(8):3311-3323.
783 doi: 10.1002/hbm.26283.
- 784 [22] Geng Z.M., Wang J., Chen G.D., Liu J.C., Lan J., Zhang Z.P., Miao J., 2023. Gut
785 microbiota and intervertebral disc degeneration: a bidirectional two-sample Mendelian

- 786 randomization study. *J Orthop Surg Res* 18(1):601. doi: 10.1186/s13018-023-04081-0.
- 787 [23] Goudman L., Demuyser T., Pilitsis J.G., Billot M., Roulaud M., Rigoard P., Moens M.,
788 2024. Gut dysbiosis in patients with chronic pain: a systematic review and meta-analysis.
789 *Front Immunol* 15:1342833. doi: 10.3389/fimmu.2024.1342833.
- 790 [24] Grasby K.L., Jahanshad N., Painter J.N., Colodro-Conde L., Bralten J., Hibar D.P., Lind
791 P.A., et al., Genetics through Meta-Analysis Consortium - Genetics working group, 2020. The
792 genetic architecture of the human cerebral cortex. *Science* 367(6484):eaay6690. doi:
793 10.1126/science.aay6690.
- 794 [25] Grundy L., Erickson A., Brierley S.M., 2019. Visceral pain. *Annu Rev Physiol* 81:
795 261-284. doi: 10.1146/annurev-physiol-020518-114525.
- 796 [26] Hartwig F.P., Smith G.D., Bowden J., 2017. Robust inference in summary data
797 Mendelian randomization via the zero modal pleiotropy assumption. *Int. J. Epidemiol.* 46,
798 1985–1998.
- 799 [27] Heiss C.N., Olofsson L.E., 2019. The role of the gut microbiota in development, function
800 and disorders of the central nervous system and the enteric nervous system. *J*
801 *Neuroendocrinol* *J Neuroendocrinol* 31(5):e12684. doi: 10.1111/jne.12684.
- 802 [28] Huang J., Zhang C., Wang J., Guo Q., Zou W., 2019. Oral *Lactobacillus reuteri* LR06 or
803 *Bifidobacterium* BL5b supplement do not produce analgesic effects on neuropathic and
804 inflammatory pain in rats. *Brain Behav* 9(4):e01260. doi: 10.1002/brb3.1260.
- 805 [29] Hui J.N., Chen Y.J., Li C.E., Gou Y.F., Liu Y., Zhou R.X., Kang M.J., Liu C., Wang B.Y.,
806 Shi P.X., Cheng S.Q., Yang X.N., Pan C.Y., Jia Y.M., Cheng B.L., Liu H., Wen Y., Zhang F.,
807 2023. Insight into the Causal Relationship between Gut Microbiota and Back Pain: A Two

808 Sample Bidirectional Mendelian Randomization Study. *Adv Genet (Hoboken)* 4(4):2300192.
809 doi: 10.1002/ggn2.202300192.

810 [30] Ivashkin V., Shifrin O., Maslennikov R., Poluektova E., Korolev A., Kudryavtseva A.,
811 Krasnov G., Benuni N., Barbara G., 2023. Eubiotic effect of rifaximin is associated with
812 decreasing abdominal pain in symptomatic uncomplicated diverticular disease: results from
813 an observational cohort study. *BMC Gastroenterol* 23(1):82. doi:
814 10.1186/s12876-023-02690-x.

815 [31] Johnston K.J.A., Ward J., Ray P.R., Adams M.J., McIntosh A.M., Smith B.H.,
816 Strawbridge R.J., Price T.J., Smith D.J., Nicholl B.I., Bailey M.E.S., 2021. Sex-stratified
817 genome-wide association study of multisite chronic pain in UK Biobank. *PLoS Genet*
818 17(4):e1009428. doi:10.1371/journal.pgen.1009428.

819 [32] Kang D., McAuley J.H., Kassem M.S., Gatt J.M., Gustin S.M., 2019. What does the grey
820 matter decrease in the medial prefrontal cortex reflect in people with chronic pain? *Eur J Pain*
821 23(2):203-219. doi: 10.1002/ejp.1304.

822 [33] Karczewski J., Troost F.J., Konings I., Dekker J., Kleerebezem M., Brummer R.J.M.,
823 Wells J.M., 2010. Regulation of human epithelial tight junction proteins by *Lactobacillus*
824 *plantarum* in vivo and protective effects on the epithelial barrier. *Am J Physiol Gastrointest*
825 *Liver Physiol* 298(6):G851-9. doi: 10.1152/ajpgi.00327.2009.

826 [34] Kozak-Szkopek E., Broczek K., Slusarczyk P., Wieczorowska-Tobis K., Klich-Raczka A.,
827 Szybalska A., Mossakowska M., 2017. Prevalence of chronic pain in the elderly polish
828 population - results of the polsenior study. *Arch Med Sci* 13(5):1197-1206. doi: 10.5114/
829 aoms.2015.55270.

- 830 [35] Kuchinad A., Schweinhardt P., Seminowicz D.A., Wood P.B., Chizh B.A., Bushnell
831 M.C.,2007. Accelerated Brain Gray Matter Loss in Fibromyalgia Patients: Premature Aging
832 of the Brain? *J Neurosci* 27(15):4004-7. doi: 10.1523/JNEUROSCI.0098-07.2007.
- 833 [36] Kurilshikov A., Medina-Gomez C., Bacigalupe R., et al., 2021. Large-scale association
834 analyses identify host factors influencing human gut microbiome composition. *Nat Genet*
835 53(2): 156-165. doi:10.1038/s41588-020-00763-1.
- 836 [37] Lawlor D.A., Harbord R.M., Sterne J.A.C., Timpson N., Smith G.D., 2008. Mendelian
837 randomization: using genes as instruments for making causal inferences in
838 epidemiology.*Stat Med* 27(8):1133-1163. doi: 10.1002/sim.3034.
- 839 [38] Lee Y.H., Song G.G., 2021. The Gut Microbiome and Osteoarthritis: A Two-Sample
840 Mendelian Randomization Study.*J Rheum Dis* 28(2):94-100. doi: 10.4078/jrd.2021.28.2.94.
- 841 [39] Li H.F., Sheng D.H., Jin C.D., Zhao G.P., Zhang L., 2023. Identifying and ranking causal
842 microbial biomarkers for colorectal cancer at different cancer subsites and stages: a
843 Mendelian randomization study. *Front Oncol* 13:1224705. doi: 10.3389/fonc.2023.1224705.
- 844 [40] Li J.S., Su S.L., Xu Z., Zhao L.H., Fan R.Y., Guo J.M., Qian D.W., Duan J.A., 2022.
845 Potential roles of gut microbiota and microbial metabolites in chronic inflammatory pain and
846 the mechanisms of therapy drugs. *Ther Adv Chronic Dis.* 28:13:20406223221091177. doi:
847 10.1177/20406223221091177.
- 848 [41] Li Y., Zhang S.X., Yin X.F., Zhang M.X., Qiao J., Xin X.H., Chang M.J., Gao C., Li Y.F.,
849 Li X.F., 2021. The Gut Microbiota and Its Relevance to Peripheral Lymphocyte
850 Subpopulations and Cytokines in Patients with Rheumatoid Arthritis. *J Immunol Res*
851 2021:6665563. doi: 10.1155/2021/6665563.

- 852 [42] Liu B., Ye D., Yang H., Song J., Sun X.H., He Z.X., Mao Y.Y., Hao G.F., 2023. Assessing
853 the relationship between GM and irritable bowel syndrome: a two-sample Mendelian
854 randomization analysis. *BMC Gastroenterology* 23(1):150. doi: 10.1186/s12876-023-02791-7.
- 855 [43] Liu J., Zhu J., Yuan F., Zhang X., Zhang Q., 2018. Abnormal brain white matter in
856 patients with right trigeminal neuralgia: a diffusion tensor imaging study. *J Headache Pain*
857 19(1):46. doi: 10.1186/s10194-018-0871-1.
- 858 [44] Lopera-Maya E.A., Kurilshikov A., van der Graaf A., Hu S.X., Andreu-Sánchez S., Chen
859 L.M., Vila A.V., Gacesa R., Sinha T., Collij V., Klaassen M.A.Y., Bolte L.A., Gois M.F.B.,
860 Neerincx P.B.T., Swertz M.A., LifeLines Cohort Study, Harmsen H.J.M., Wijmenga C., Fu
861 J.Y., Weersma R.K., Zhernakova A., Sanna S., 2022. Effect of host genetics on the gut
862 microbiome in 7,738 participants of the Dutch microbiome project. *Nat Genet* 54(2):143-151.
863 doi: 10.1038/s41588-021-00992-y.
- 864 [45] Luczynski P., Tramullas M., Viola M., Shanahan F., Clarke G., O'Mahony S., Dinan T.G.,
865 Cryan J.F., 2017. Microbiota regulates visceral pain in the mouse. *Elife* 6:e25887. doi:
866 10.7554/eLife.25887.
- 867 [46] Martucci K.T., MacKey S.C., 2018. Neuroimaging of Pain: Human Evidence and
868 Clinical Relevance of Central Nervous System Processes and Modulation. *Anesthesiology*
869 128(6):1241-1254. doi: 10.1097/ALN.0000000000002137.
- 870 [47] Mayer E.A., Gupta A., Kilpatrick L.A., Hong J.Y., 2015. Imaging brain mechanisms in
871 chronic visceral pain. *Pain* 156 Suppl 1(0 1):S50-S63. doi:
872 10.1097/j.pain.000000000000106.
- 873 [48] Melzack R., 2001. Pain and the neuromatrix in the brain. *J Dent Educ* 65(12):1378-1382.

- 874 [49] Meng W., Adams M.J., Reel P., Rajendrakumar A., Huang Y., Deary I.J., Palmer C.N.A.,
875 McIntosh A.M., Smith B.H.,2020. Genetic correlations between pain phenotypes and
876 depression and neuroticism. *Eur J Hum Genet* 28(3):358-366. doi:
877 10.1038/s41431-019-0530-2.
- 878 [50] Minerbi A., Shen S., 2022. Gut microbiome in anesthesiology and pain medicine.
879 *Anesthesiology* 137(1):93-108. doi:10.1097/ALN.0000000000004204.
- 880 [51] Mutso A.A., Radzicki D., Baliki M.N., Huang L., Banisadr G., Centeno M.V., Radulovic
881 J., Martina M., Miller R.J., Apkarian A.V.,2012. Abnormalities in hippocampal functioning
882 with persistent pain.*J Neurosci* 32(17):5747-56. doi: 10.1523/JNEUROSCI.0587-12.2012.
- 883 [52] Ng S.K., Urquhart D.M., Fitzgerald P.B., Cicuttini F.M., Hussain S.M., Fitzgibbon
884 B.M.,2018.The Relationship Between Structural and Functional Brain Changes and Altered
885 Emotion and Cognition in Chronic Low Back Pain Brain Changes A Systematic Review of
886 MRI and fMRI Studies. *Clin J Pain* 34(3):237-261. doi: 10.1097/AJP.0000000000000534.
- 887 [53] O'Mahony S.M., Dinan T.G., Cryan J.F.,2017. The gut microbiota as a key regulator of
888 visceral pain. *Pain* 158 Suppl 1:S19-S28. doi: 10.1097/j.pain.0000000000000779.
- 889 [54] Oh D.K., Na H.S., Jhun J.Y. Lee J.S., Um I.G., Lee S.Y., Park M.S., Cho M.L., Park
890 S.H.,2023. Bifidobacterium longum BORI inhibits pain behavior and chondrocyte death, and
891 attenuates osteoarthritis progression. *PLoS One* 18(6):e0286456. doi:
892 10.1371/journal.pone.0286456.
- 893 [55] Ostrowsky K., Magnin M., Rylvlin P., Isnard J., Guenot M., Mauguiere F.,
894 2002.Representation of pain and somatic sensation in the human insula: A study of responses
895 to direct electrical cortical stimulation. *Cereb Cortex* 12(4):376-85. doi:

- 896 10.1093/cercor/12.4.376.
- 897 [56] Palmer T.M., Sterne J.A.C., Harbord R.M., Lawlor D.A., Sheehan N.A., Meng S.,
898 Granel R., Smith G.D., Didelez V., 2011. Instrumental variable estimation of causal risk
899 ratios and causal odds ratios in Mendelian randomization analyses. *Am. J. Epidemiol.* 173,
900 1392-1403.
- 901 [57] Pang J.C., Aquino K.M., Oldehinkel M., Robinson P.A., Fulcher B.D., Breakspear M.,
902 Fornito A., 2023. Geometric constraints on human brain function. *Nature* 618(7965):566-574.
903 doi: 10.1038/s41586-023-06098-1.
- 904 [58] Ploghaus A., Tracey I., Gati J.S., Clare S., Menon R.S., Matthews P.M., Rawlins J.N.,
905 1999. Dissociating pain from its anticipation in the human brain. *Science* 284(5422):1979-81.
906 doi: 10.1126/science.284.5422.1979.
- 907 [59] Pratt C., Campbell M.D., 2020. The Effect of Bifidobacterium on Reducing Symptomatic
908 Abdominal Pain in Patients with Irritable Bowel Syndrome: A Systematic Review. *Probiotics*
909 *Antimicrob Proteins* 12(3):834-839. doi: 10.1007/s12602-019-09609-7.
- 910 [60] Qin Y.W., Havulinna A.S., Liu Y., Jousilahti P., Ritchie S.C., Tokolyi A., Sanders J.G.,
911 Valsta L., Brożyńska M., Zhu Q.Y., Tripathi A., Vázquez-Baeza Y., Loomba R., Cheng S.S.,
912 Jain M., Niiranen T., Lahti L., Knight R., Salomaa V., Inouye M., Méric G., 2022. Combined
913 effects of host genetics and diet on human gut microbiota and incident disease in a single
914 population cohort. *Nat Genet* 54(2):134-142. doi: 10.1038/s41588-021-00991-z.
- 915 [61] Ramakrishna C., Corleto J., Ruegger P.M., Logan G.D., Peacock B.B., Mendonca S.,
916 Yamaki S., Adamson T., Ermel R., McKemy D., Borneman J., Cantin E.M., 2019. Dominant
917 role of the gut microbiota in chemotherapy induced neuropathic pain. *Sci Rep* 9(1):20324. doi:

- 918 10.1038/s41598-019-56832-x.
- 919 [62] Ran Guo, Li-Hua Chen, Chungen Xing, Tong Liu, 2019. Pain regulation by gut
920 microbiota: molecular mechanisms and therapeutic potential. *Br J Anaesth* 123 (5): 637-654.
921 doi: 10.1016/j.bja.2019.07.026.
- 922 [63] Ren M., Lotfipour S., 2020. The role of the gut microbiome in opioid use, *Behav*
923 *Pharmacol* 31(2&3):113-121. doi: 10.1097/FBP.0000000000000538.
- 924 [64] Rodriguez-Raecke R., Niemeier A., Ihle K., Ruether W., May A., 2009. Brain Gray
925 Matter Decrease in Chronic Pain Is the Consequence and Not the Cause of Pain. *J Neurosci*
926 29(44):13746-50. doi: 10.1523/JNEUROSCI.3687-09.2009
- 927 [65] Rühlemann M.C., Hermes B.M., Bang C., Doms S., Moitinho-Silva L., Thingholm L.B.,
928 Frost F., Degenhardt F., Wittig M., Kässens J., Weiss F.U., Peters A., Neuhaus K., Völker
929 U., Völzke H., Homuth G., Weiss S., Grallert H., Laudes M., Lieb W., Haller D.,
930 Lerch M.M., Baines J.F., Franke A., 2021. Genome-wide association study in 8,956
931 German individuals identifies influence of ABO histo-blood groups on gut microbiome. *Nat*
932 *Genet* 53(2):147-155. doi: 10.1038/s41588-020-00747-1.
- 933 [66] Russo R., Cristiano C., Avagliano C., Caro C.D., Rana G.L., Raso G.M., Canani R.B.,
934 Meli R., Calignano A., 2018. Gut-brain axis: role of lipids in the regulation of inflammation,
935 pain and CNS diseases. *Curr Med Chem* 25(32):3930-3952. doi:
936 10.2174/0929867324666170216113756.
- 937 [67] Sanderson E., 2021. Multivariable Mendelian randomization and mediation. *Cold Spring*
938 *Harb Perspect Med* 11(2):a038984. <https://doi.org/10.1101/cshperspect.a038984>.
- 939 [68] Sawamoto N., Honda M., Okada T., Hanakawa T., Kanda M., Fukuyama H., Konishi J.,

- 940 Shibusaki H.,2000. Expectation of painenhances responses to nonpainful somatosensory
941 stimulation in the anterior cingulate cortex and parietal operculum/posterior insula: An
942 event-related functional magnetic resonance imaging study. *J Neurosci* 20(19):7438-45. doi:
943 10.1523/JNEUROSCI.20-19-07438.2000.
- 944 [69] Schermuly I., Fellgiebel A., Wagner S., Yakushev I., Stoeter P., Schmitt R., Knickenberg
945 R.J., Bleichner F., Beutel M.E., 2010. Association between cingulum bundle structure and
946 cognitive performance: an observational study in major depression.*Eur Psychiatry*
947 25(6):355-60. doi: 10.1016/j.eurpsy.2010.05.001.
- 948 [70] Schmidt-Wilcke T., Ganssbauer S., Neuner T., Bogdahn U., May A.,2008. Subtle grey
949 matter changes between migraine patients and healthy controls. *Cephalalgia* 28(1):1-4. doi:
950 10.1111/j.1468-2982.2007.01428.x.
- 951 [71] Seminowicz D.A., Labus J.S., Bueller J.A., Tillisch K., Naliboff B.D., Bushnell M.C.,
952 Mayer E.A.,2010. Regional Gray Matter Density Changes in Brains of Patients With Irritable
953 Bowel Syndrome. *Gastroenterology* 139(1):48-57.e2. doi: 10.1053/j.gastro.2010.03.049.
- 954 [72] Seminowicz D.A., Moayed M.,2017. The Dorsolateral Prefrontal Cortex in Acute and
955 Chronic Pain. *J Pain* 18(9):1027-1035. doi: 10.1016/j.jpain.2017.03.008.
- 956 [73] Shiers S., Price T.J.,2020.Molecular, circuit, and anatomical changes in the prefrontal
957 cortex in chronic pain. *Pain*. 161(8):1726-1729. doi: 10.1097/j.pain.000000000000189745.
- 958 [74] Silvestre M.P., Rodrigues A.M., Canhão H., Marques C., Teixeira D., Calhau C., Branco
959 J., 2020. Cross-talk between diet-associated dysbiosis and hand osteoarthritis. *Nutrients*
960 12(11):3469. doi: 10.3390/nu12113469.
- 961 [75] Smith S.M., Douaud G., Chen W., Hanayik T., AlfaroAlmagro F., Sharp K., Elliott L.T.,

- 962 2021. An expanded set of genome-wide association studies of brain imaging phenotypes in
963 UK Biobank. *Nat Neurosci* 24(5):737-745. doi: 10.1038/s41593-021-00826-4.
- 964 [76] Sommer F., Bäckhed F., 2013. The gut microbiota--masters of host development and
965 physiology. *Nat Rev Microbiol* 11(4):227-38. doi: 10.1038/nrmicro2974.
- 966 [80] Storey J.D., 2003. The positive false discovery rate: A Bayesian interpretation and the
967 q-value. *Ann. Stat.* 31(6):2013–2035. DOI: 10.1214/aos/1074290335.
- 968 [77] Su M.C., Tang Y.D., Kong W.S., Zhang S.Y., Zhu T, 2023. Genetically supported
969 causality between gut microbiota, gut metabolites and low back pain: a two-sample
970 Mendelian randomization study. *Front Microbiol* 14:1157451. doi:
971 10.3389/fmicb.2023.1157451.
- 972 [78] Theodorou V., Ait Belgnaoui A., Agostini S., Eutamene H., 2014. Effect of commensals
973 and probiotics on visceral sensitivity and pain in irritable bowel syndrome. *Gut Microbe*
974 5(3):430-436. doi: 10.4161/gmic.29796.
- 975 [79] Thomas A.G., Koumellis P., Dineen R.A., 2011. The Fornix in Health and Disease: An
976 Imaging Review. *Radiographics*. 31(4):1107-21. doi: 10.1148/rg.314105729.
- 977 [80] Timmers I., Biggs E.E., Bruckert L., Tremblay-McGaw A.G., Zhang H., Borsook D.,
978 Simons L.E., 2024. Probing white matter microstructure in youth with chronic pain and its
979 relation to catastrophizing using neurite orientation dispersion and density imaging. *Pain* 8.
980 doi: 10.1097/j.pain.0000000000003269.
- 981 [81] Treede R.D, Rief W., Barke A., Aziz Q., Bennett M.I., Benoliel R., Cohen M., Evers S.,
982 [82] Finnerup N.B., First M.B., Giamberardino M.A., Kaasa S., Kosek E., Lavand'homme P.,
983 Nicholas M., Perrot S., Scholz J., Schug S., Smith B.H., Svensson P., Vlaeyen J.W.S., Wang

- 984 Shuu-Jiun, 2015. A classification of chronic pain for ICD-11. *Pain* 156(6):1003-1007. doi:
985 10.1097/j.pain.000000000000160.
- 986 [83] Vachon-Presseau E., Centeno M.V., Ren W., Berger S.E., Tetreault P., Ghantous M.,
987 Baria A., Farmer M., Baliki M.N., Schnitzer T.J., Apkarian A.V., 2016. The Emotional Brain
988 as a Predictor and Amplifier of Chronic Pain. *J Dent Res* 95(6):605-12. doi:
989 10.1177/0022034516638027.
- 990 [84] Verbanck M., Chen C.Y., Neale B., D R., 2018. Detection of widespread horizontal
991 pleiotropy in causal relationships inferred from Mendelian randomization between complex
992 traits and diseases. *Nat Genet.* 50 (5), 693–698.
- 993 [85] Wang S., Zang M., Yang X., Lv L., Chen L., Cui J., Liu Y., Xia Y., Zhou N., Yang Z., Li
994 Y., Shi B., 2023. Gut microbiome in men with chronic prostatitis/chronic pelvic pain
995 syndrome: profiling and its predictive significance. *World J Urol* 41(11):3019-3026. doi:
996 10.1007/s00345-023-04587-6.
- 997 [86] Wang X., Wu Y., Liu Y., Chen F., Chen S., Zhang F., Li S., Wang C., Gong Y., Huang R.,
998 Hu M., Ning Y., Zhao H., Guo X., 2023. Altered gut microbiome profile in patients with
999 knee osteoarthritis. *Front Microbiol* 14:1153424. doi: 10.3389/fmicb.2023.1153424.
- 1000 [87] Wu R., Wang D., Cheng L., Su R., Li B., Fan C., Gao C., Wang C., 2024. Impaired
1001 immune tolerance mediated by reduced Tfr cells in rheumatoid arthritis linked to gut
1002 microbiota dysbiosis and altered metabolites. *Arthritis Res Ther* 26(1):21. doi:
1003 10.1186/s13075-023-03260-y.
- 1004 [88] Wu Z., Liu H., Yan E., Zhang X., Wang Y., Huang C., He T., Miao L., Yang L., Jiang R.,
1005 Qi C., Liu C., Wang D., Yang C., 2023. *Desulfovibrio* confers resilience to the comorbidity of

- 1006 pain and anxiety in a mouse model of chronic inflammatory pain. *Psychopharmacology (Berl)*
1007 240(1):87-100. doi: 10.1007/s00213-022-06277-4.
- 1008 [89] Xiao X., Ding M., Zhang Y.Q.,2021. Role of the Anterior Cingulate Cortex in
1009 Translational Pain Research.*Neurosci Bull* 37(3):405-422. doi: 10.1007/s12264-020-00615-2.
- 1010 [90] Yang M.Y., Wan X.J., Zheng H.S., Xu K., Xie J.L., Yu H., Wang J.C., Xu P., 2023. No
1011 Evidence of a Genetic Causal Relationship between Ankylosing Spondylitis and Gut
1012 Microbiota: A Two-Sample Mendelian Randomization Study.*Nutrients* 15(4):1057. doi:
1013 10.3390/nu15041057.
- 1014 [91] Yang S., Chang M.C., 2019.Chronic Pain: Structural and Functional Changes in Brain
1015 Structures and Associated Negative Affective State.*Int J Mol Sci* ,20(13):3130. doi:
1016 10.3390/ijms20133130.
- 1017 [92] Ye T., Shao J., Kang H., 2021. Debiased Inverse-Variance Weighted Estimator in
1018 Two-Sample Summary-Data Mendelian Randomization. *The Annals of Statistics*, 49(4),
1019 2079-2100. <https://arxiv.org/abs/1911.09802>.
- 1020 [93] Yin Q.Y., Zhu L., 2024. Does co-localization analysis reinforce the results of Mendelian
1021 randomization? *Brain* 147(1):e7-e8. doi: 10.1093/brain/awad295.
- 1022 [94] Yu X.H., Yang Y.Q., Cao R.R., Bo L., Lei S.F., 2021. The causal role of gut microbiota in
1023 development of osteoarthritis.*Osteoarthritis Cartilage* 29(12):1741-1750. doi:
1024 10.1016/j.joca.2021.08.003.
- 1025 [95] Zhao J., Ming J., Hu X.H., Chen G., Liu J., Yang C., 2020. Bayesian weighted Mendelian
1026 randomization for causal inference based on summary statistics. *Bioinformatics*
1027 36(5):1501–1508. <https://doi.org/10.1093/bioinformatics/btz749>.

1028 [96] Zhao Q., Wang J., Hemani G., Bowden J., Small D.S., 2020. Statistical inference in
1029 two-sample summary-data Mendelian randomization using robust adjusted profile score. Ann
1030 Statist 48(3):1742-1769.<https://arxiv.org/abs/1801.09652>.

1031 [97] Zhou R., Zhang L., Sun Y., Yan J., Jiang H., 2023. Causal Associations between Dietary
1032 Habits and Chronic Pain: A Two-Sample Mendelian Randomization Study. Nutrients
1033 15(17):3709. doi: 10.3390/nu15173709.

1034

1035

1036

1037

1038

1039

1040

1041

1042

1043

1044

1045

1046

1047

1048

1049

1050

1051

1052

1053

1054

1055

1056

1057

1058

1059

Table 1 Description of GWAS summary statistics used for each phenotype.

Phenotype	First author (year)	Consortium	Sample size	Population
MCP	Johnston (2019)	UK Biobank	387,649 participants	European
Headache	Meng (2020)	UK Biobank	74,761 cases and	European

			149,312 controls	
Facial pain			2,610 cases and 149,312 controls	European
Neck/shoulder pain			53,994 cases and 149,312 controls	European
Abdominal pain			8,217 cases and 149,312 controls	European
Back pain			4,3991 cases and 149,312 controls	European
Hip pain			10,116 cases and 149,312 controls	European
Knee pain			22,204 cases and 149,312 controls	European
Pain all over body			5,670 cases and 149,312 controls	European
Gut microbiota	Esteban A. Lopera-Maya (2022)	NA	7,738 participants	European
	Youwen Qin (2022)	FINRISK 2002 study	5,959 participants	European
	Malte Christoph Rühlemann (2021)	NA	8,956 participants	European
	Alexander Kurilshikov (2021)	NA	13,266 participants	European
Brain imaging-derived phenotypes	Stephen M Smith (2021)	UK Biobank	39,691 participants	European
Human cerebral cortex	Katrina L. Grasby (2020)	ENIGMA	51,665 participants	European
83 brain-wide volumes	Fürtjes, A. E. (2023)	UK Biobank	36,778 participants	European

1060 Abbreviation: MCP: multi-site chronic pain; ENIGMA: Enhancing NeuroImaging

1061 Genetics through Meta-Analysis Consortium.

Table 2: Mendelian randomization results of positive gut microbiota abundance based on Meta analysis on MCP and 8 pain phenotypes

Scoure	outcome	exposure	method	n SNP	pval	or	or_lci95	or_uci95	Heterogeneity (Q_pval)	Pleiotropy (pval)	MR-Presso (pval)	Global Test (pval)	pval-Meta (after meta analysis for IVW)	
Data3: Esteban A. Lopera-Maya(2022)	MCP	Phylum Verrucomicrobia	Inverse variance weighted	15	0.01896235	0.982081572	0.967359461	0.997027737	0.320706194	0.996488375	0.034205687	0.356	0.011212335	
			MR Egger	15	0.705456547	0.981876022	0.894877276	1.077332667	0.255626493					
			Weighted median	15	0.057206847	0.981224799	0.962243091	1.00058095						
			Weighted mode	15	0.239122587	0.979740585	0.948291179	1.012232988						
			Contamination mixture method	15	0.025678249	0.979175831	0.964597802	0.993974179						
			Robust adjusted profile score (RAPS)	15	0.013364658	0.98072196	0.965712745	0.99596445						
			Debiased inverse-variance weighted method	15	0.015269901	0.98123824	0.966337206	0.996369049						
			Constrained maximum likelihood	15	0.066550807	0.982169094	0.963471499	1.001229543						
			Bayesian Weighted Mendelian Randomization	15	0.022821328	0.981130186	0.965168726	0.997355609						
	Genus Adlercreutzia	Inverse variance weighted	7	0.037093537	1.017400871	1.001032702	1.034036681	0.715183867	0.401707082	0.038058782	0.7226667	0.022358123		
		MR Egger	7	0.192938083	1.041980755	0.987605133	1.099350192	0.71909744						
		Weighted median	7	0.058954708	1.020411518	0.999235622	1.042036176							
		Weighted mode	7	0.189889788	1.025196018	0.991917237	1.0595913							
		Contamination mixture method	7	0.054339369	1.023329817	1.003066529	1.04400245							
		Robust adjusted profile score	7	0.053479635	1.017814924	0.9997351	1.036221714							

			(RAPS)											
			Debiased inverse-variance weighted method	7	0.040380183	1.018270112	1.000793815	1.036051587						
			Constrained maximum likelihood	7	0.057065151	1.017608502	0.999475524	1.036070457						
			Bayesian Weighted Mendelian Randomization	7	0.045085083	1.017709777	1.000384307	1.035335303						
Data1:Alexander Kurilshikov (2021)	headache	Phylum Verrucomicrobia	Inverse variance weighted	12	0.02014992	0.985462476	0.973363963	0.99771137	0.58688606	0.561706706	0.028666522	0.6193333	0.023188736	
			MR Egger	12	0.785329636	0.995130931	0.961681908	1.029743371	0.530259011					
			Weighted median	12	0.106858612	0.985795464	0.968800933	1.00308811						
			Weighted mode	12	0.219111487	0.983304873	0.958719669	1.008520535						
			Contamination mixture method	12	0.008827096	0.980101247	0.970349076	0.989951428						
			Robust adjusted profile score (RAPS)	12	0.015016258	0.983264178	0.969980401	0.996729875						
			Debiased inverse-variance weighted method	12	0.02170849	0.984773151	0.971955041	0.997760305						
			Constrained maximum likelihood	12	0.045058541	0.984113094	0.968819988	0.999647607						
			Bayesian Weighted Mendelian Randomization	12	0.019146516	0.984285304	0.971327448	0.997416023						
Data4:Youwen Qin (2022)	facialpain	Genus Alistipes	Inverse variance weighted	17	0.011651233	1.004199247	1.000934924	1.007474215	0.474966723	0.538356301	0.021510576	0.5016667	0.046806403	
			MR Egger	17	0.537663714	1.0022328	0.995311407	1.009202324	0.431189248					
			Weighted median	17	0.189311535	1.003137479	0.998456215	1.00784069						
			Weighted mode	17	0.80601021	1.000789299	0.994610039	1.007006948						

			Contamination mixture method	17	1	1.005532274	1.005532274	1.005532274						
			Robust adjusted profile score (RAPS)	17	0.024136725	1.004095569	1.000534747	1.007669063						
			Debiased inverse-variance weighted method	17	0.012698904	1.004400835	1.000938026	1.007875624						
			Constrained maximum likelihood	17	0.039775642	1.004207257	1.000196194	1.008234405						
			Bayesian Weighted Mendelian Randomization	17	0.014207917	1.00447811	1.000896887	1.008072146						
	Genus													
	Bifidobacterium		Inverse variance weighted	16	0.014300484	1.004167659	1.000831637	1.007514802	0.626808686	0.772838386	0.01768728	0.668	0.044816124	
			MR Egger	16	0.455993731	1.003090012	0.995209617	1.011032806	0.558563741					
			Weighted median	16	0.152348849	1.003594074	0.998675608	1.008536764						
			Weighted mode	16	0.552709661	1.002031766	0.99548966	1.008616865						
			Contamination mixture method	16	0.127246974	1.008339777	1.003310661	1.013394101						
			Robust adjusted profile score (RAPS)	16	0.023488461	1.004226444	1.000568722	1.007897536						
			Debiased inverse-variance weighted method	16	0.015670281	1.00437376	1.000824792	1.007935313						
			Constrained maximum likelihood	16	0.02392076	1.004198498	1.000553734	1.007856539						
			Bayesian Weighted Mendelian Randomization	16	0.017127221	1.004392469	1.000779751	1.008018227						
Data2:Malte														
Christoph Rühlemann	neckshoulderpa	Class												
(2021)	in	Alphaproteobacteria	Inverse variance weighted	9	0.049427264	0.992671151	0.985414044	0.999981703	0.664447486	0.484943501	0.05058963	0.679	0.011661252	

			MR Egger	9	0.28445787	0.980833171	0.949252346	1.013464662	0.62307216				
			Weighted median	9	0.023221186	0.98882251	0.979271083	0.998467098					
			Weighted mode	9	0.161788776	0.987787362	0.972473302	1.003342582					
			Contamination mixture method	9	0.025093216	0.98983035	0.984893551	0.994791896					
			Robust adjusted profile score (RAPS)	9	0.063302791	0.992397015	0.984435271	1.000423151					
			Debiased inverse-variance weighted method	9	0.052076005	0.992315926	0.98462249	1.000069476					
			Constrained maximum likelihood	9	0.077646356	0.992485038	0.984203677	1.000836082					
			Bayesian Weighted Mendelian Randomization	9	0.057327506	0.992487255	0.984799649	1.000234872					
Data3: Esteban A. Lopera-Maya(2022)	neckshoulderpa in	Genus Odoribacter	Inverse variance weighted	11	0.000120392	0.980127005	0.970149998	0.990206616	0.393943934	0.555697627	0.00323682	0.4533333	5.54E-05
			MR Egger	11	0.162045887	0.967679887	0.927623131	1.009466379	0.340467459				
			Weighted median	11	0.053994863	0.98629622	0.972549527	1.000237219					
			Weighted mode	11	0.300401396	0.98699109	0.964066825	1.010460464					
			Contamination mixture method	11	0.007229237	0.97100033	0.956544019	0.985675121					
			Robust adjusted profile score (RAPS)	11	0.000230236	0.979284948	0.968437306	0.990254097					
			Debiased inverse-variance weighted method	11	0.000140566	0.979169955	0.968616033	0.989838871					
			Constrained maximum likelihood	11	0.000765214	0.980860944	0.969882614	0.99196354					
			Bayesian Weighted Mendelian Randomization	11	0.000227424	0.979176678	0.96828247	0.990193458					

Data2:Malte																				
Christoph Rühlmann (2021)	abdominalpain	Class	Inverse variance weighted	12	0.030973525	1.005120662	1.000467477	1.00979549	0.257858001	0.104285968	0.053022345	0.4586667	0.019528997							
		Gammaproteobacteria																		
		MR Egger												12	0.038938744	1.020021487	1.003470424	1.036845541	0.41590708	
		Weighted median												12	0.070074263	1.006186368	0.999494298	1.012923244		
		Weighted mode												12	0.183251476	1.009335192	0.99647498	1.022361375		
		Contamination mixture method												12	0.057007608	1.006511955	1.001491956	1.011557117		
		Robust adjusted profile score (RAPS)												12	0.035110906	1.005738824	1.000399513	1.011106631		
		Debiased inverse-variance weighted method												12	0.033133464	1.00538201	1.000429562	1.010358973		
		Constrained maximum likelihood												12	0.079473129	1.005133531	0.999398	1.010901978		
		Bayesian Weighted Mendelian Randomization												12	0.038580029	1.00536023	1.00028079	1.010465463		
Data3: Esteban A. Lopera-Maya(2022)	abdominalpain	Specie	Inverse variance weighted	14	0.037170702	1.005438062	1.000322462	1.010579824	0.502554055	0.221626957	0.051738488	0.515	0.011809517							
Eubacterium_eligens																				
MR Egger		14												0.10869721	1.019849581	0.997428279	1.042774893	0.5594664		
Weighted median		14												0.505238304	1.002367504	0.995418862	1.009364651			
Weighted mode		14												0.837825764	1.001287055	0.98927152	1.013448529			
Contamination mixture method		14												1	1.000623339	0.99066697	1.01067977			
Robust adjusted profile score (RAPS)		14												0.051240949	1.005532469	0.999970161	1.011125717			
Debiased inverse-variance weighted method		14												0.038767366	1.00570398	1.000293556	1.011143669			
Constrained maximum		14												0.093423765	1.005277789	0.999114315	1.011479285			

			likelihood										
			Bayesian Weighted Mendelian	14	0.040918523	1.005642054	1.000232176	1.011081192					
			Randomization										
Data4:Youwen Qin (2022)	abdominalpain	Genus Alistipes	Inverse variance weighted	17	0.034563673	0.994119526	0.988696879	0.999571914	0.595696913	0.491111695	0.038413382	0.574	0.037071944
			MR Egger	17	0.708480803	0.997760439	0.98632101	1.009332543	0.560486256				
			Weighted median	17	0.048097332	0.992333679	0.984789425	0.999935728					
			Weighted mode	17	0.127483607	0.990001778	0.977946691	1.002205467					
			Contamination mixture method	17	0.034975212	0.991745545	0.986799194	0.99671669					
			Robust adjusted profile score (RAPS)	17	0.044606378	0.993596395	0.987386484	0.999845361					
			Debiased inverse-variance weighted method	17	0.03613241	0.993838748	0.988110081	0.999600628					
			Constrained maximum likelihood	17	0.121487814	0.994274893	0.987075638	1.001526656					
			Bayesian Weighted Mendelian Randomization	17	0.032859932	0.993535441	0.98763423	0.999471912					
Data2:Malte Christoph Rühle (2021)	backpain	Family Prevotellaceae	Inverse variance weighted	10	0.011517883	0.987829799	0.978490852	0.997257879	0.891323316	0.530430988	0.005238675	0.8936667	0.051986091
			MR Egger	10	0.297118662	0.971426794	0.923174937	1.022200644	0.869537076				
			Weighted median	10	0.029422081	0.98696447	0.975377877	0.9986887					
			Weighted mode	10	0.378620097	0.990542242	0.970817122	1.010668138					
			Contamination mixture method	10	0.020401764	0.980987337	0.971226349	0.990846423					
			Robust adjusted profile score (RAPS)	10	0.020085431	0.987569712	0.977209839	0.998039415					

Data3: Esteban A. Lopera-Maya(2022)	backpain	Order Bifidobacteriales	Debiased inverse-variance weighted method	10	0.012991938	0.987238155	0.977283441	0.997294269						
			Constrained maximum likelihood	10	0.008733108	0.987475255	0.978216471	0.996821674						
			Bayesian Weighted Mendelian Randomization	10	0.014859254	0.987611206	0.977753888	0.997567903						
			Inverse variance weighted	10	0.024781716	1.012196355	1.001539132	1.022966979	0.526108983	0.63667517	0.041967538	0.5563333	0.048289803	
			MR Egger	10	0.966149481	1.001018758	0.956415205	1.04770245	0.449356295					
			Weighted median	10	0.413260679	1.006131903	0.99150478	1.020974812						
			Weighted mode	10	0.802039262	1.002851983	0.981406648	1.024765934						
	Contamination mixture method	10	0.308472923	1.008921833	0.984011464	1.034462811								
	Robust adjusted profile score (RAPS)	10	0.042078684	1.012099554	1.000430474	1.023904743								
	Debiased inverse-variance weighted method	10	0.026789964	1.012802431	1.001463371	1.024269877								
	Constrained maximum likelihood	10	0.047783882	1.012384076	1.000119932	1.024798611								
	Bayesian Weighted Mendelian Randomization	10	0.026833505	1.01280865	1.001460851	1.024285035								
	Data3: Esteban A. Lopera-Maya(2022)	hippain	Genus Subdoligranulum	Inverse variance weighted	14	0.040941121	0.994016288	0.988312462	0.999753032	0.695222364	0.93872199	0.036393135	0.7083333	0.084123458
				MR Egger	14	0.595713927	0.993044007	0.968427048	1.018286718	0.617883741				
Weighted median				14	0.133654032	0.994184607	0.986635995	1.001790972						
Weighted mode				14	0.481602733	0.995351087	0.982882144	1.007978212						
Contamination mixture method				14	0.033443546	0.98834282	0.983413439	0.993296909						

Data3: Esteban A. Lopera-Maya(2022)	kneepain	Genus Dialister	Robust adjusted profile score (RAPS)	14	0.039933534	0.993417293	0.987177566	0.99969646						
			Debiased inverse-variance weighted method	14	0.042583569	0.993725818	0.987698746	0.999789668						
			Constrained maximum likelihood	14	0.072849614	0.993995135	0.987475018	1.000558302						
			Bayesian Weighted Mendelian Randomization	14	0.045143324	0.993833092	0.987836335	0.999866253						
			Inverse variance weighted	6	0.039429035	0.991862294	0.984179924	0.999604631	0.943919259	0.544618433	0.008596778	0.9403333	0.076926359	
			MR Egger	6	0.38423355	0.975621289	0.92845471	1.025183984	0.942064135					
			Weighted median	6	0.048935567	0.990713773	0.981556343	0.999956637						
			Weighted mode	6	0.173568213	0.988647944	0.974797939	1.00269473						
			Contamination mixture method	6	0.058228668	0.987208205	0.982284483	0.992156607						
			Robust adjusted profile score (RAPS)	6	0.062481149	0.991780812	0.983205976	1.000430431						
			Debiased inverse-variance weighted method	6	0.04321034	0.991468413	0.983266579	0.999738661						
			Constrained maximum likelihood	6	0.060032881	0.992238042	0.984212276	1.000329254						
Bayesian Weighted Mendelian Randomization	6	0.04728183	0.991746348	0.983658485	0.99990071									
Data1:Alexander Kurilshikov (2021)	pain all over body	Genus Desulfovibrio	Inverse variance weighted	10	0.007007636	0.990925643	0.984381459	0.997513334	0.259825515	0.228982182	0.024534683	0.2926667	0.014860797	
			MR Egger	10	0.063949596	0.978887778	0.96001468	0.998131906	0.319972357					
			Weighted median	10	0.518084294	0.997200376	0.988757955	1.005714882						

		Weighted mode	10	0.871703393	0.998864675	0.985569477	1.012339223					
		Contamination mixture method	10	0.458119132	0.984551043	0.969892988	0.999430627					
		Robust adjusted profile score (RAPS)	10	0.009518935	0.990624166	0.983595075	0.997703489					
		Debiased inverse-variance weighted method	10	0.004553699	0.990478095	0.983952743	0.997046723					
		Constrained maximum likelihood	10	0.014943969	0.990999745	0.983810341	0.998241688					
		Bayesian Weighted Mendelian Randomization	10	0.005742703	0.990060955	0.983068192	0.997103459					
pain all over body	Genus Ruminococcus2	Inverse variance weighted	15	0.001458371	1.009788338	1.003749387	1.015863622	0.994893032	0.864546703	3.95E-05	0.9946667	0.002812313
		MR Egger	15	0.204084459	1.011142252	0.994852529	1.027698703	0.990527392				
		Weighted median	15	0.008701806	1.010442011	1.002630768	1.018314108					
		Weighted mode	15	0.04276989	1.014346053	1.001716297	1.027135046					
		Contamination mixture method	15	0.001937794	1.010483869	1.00544406	1.015548941					
		Robust adjusted profile score (RAPS)	15	0.003823886	1.009934287	1.003191569	1.016722324					
		Debiased inverse-variance weighted method	15	0.001804249	1.010271901	1.003808221	1.016777201					
		Constrained maximum likelihood	15	0.00446083	1.009941646	1.003078649	1.0168516					
		Bayesian Weighted Mendelian Randomization	15	0.002196357	1.010056697	1.003608425	1.0165464					

Table 3: genetic colocalisation analysis results of positive gut microbiota abundance based on
Meta analysis on MCP and 8 pain phenotypes

Scoure	outcome	exposure	nsn p	PP.H4.abf
Data3: Esteban A. Lopera-Maya(2022)	MCP	Phylum Verrucomicrobia	258	0.0018262 13
		Genus Adlercreutzia	130	0.0016919 34
Data1:Alexander Kurilshikov (2021)	headache	Phylum Verrucomicrobia	178	/
Data4:Youwen Qin (2022)	facialpain	Genus Alistipes	249	0.0422121 55
		Genus Bifidobacterium	188	0.0555433 83
Data3: Esteban A. Lopera-Maya(2022)	neckshoulder pain	Genus Odoribacter	225	0.0520624 98
Data2:Malte Christoph Rühlemann (2021)	abdominalpain	Class Gammaproteobacteria		
Data3: Esteban A. Lopera-Maya(2022)	abdominalpain	Specie Eubacterium_eligens	415	0.0225092 93
Data4:Youwen Qin (2022)	abdominalpain	Genus Alistipes	249	0.0558042 56
Data2:Malte Christoph Rühlemann (2021)	backpain	Family Prevotellaceae		
Data3: Esteban A. Lopera-Maya(2022)	backpain	Order Bifidobacteriales	42	0.0060220 88
Data3: Esteban A. Lopera-Maya(2022)	hippain	Genus Subdoligranulum	333	0.0144852 39
Data3: Esteban A. Lopera-Maya(2022)	kneepain	Genus Dialister	205	0.0173670 48
Data1:Alexander Kurilshikov (2021)	pain all over body	Genus Desulfovibrio	210	0.0128547 44
		Genus Ruminococcus2	242	0.0188889 71

MCP : multisite chronic pain

1064
1065
1066
1067

1068

1069

1070

1071

1072

1073

Table 4 Three causal effects (a, b, c') of the mediation analysis in IVW method

Causal	effects:	nSNP	Value*	P
Exposure-mediating				
variable-outcome				
Genus Odoribacter- mean OD in		11	a=0.111738712832827	0.00014925
Fornix cres+Stria terminalis		9	b=-0.025127303642184	0.006414495
(left)- neck/shoulder pain		11	c'=-0.0200731182675427	0.000120392

1074

1075

1076

nSNP: number of SNP; *a: exposure to mediating variable causal effects; b: mediating variable to outcome causal effects; c': exposure to outcome variable causal effects exposure-mediating variable-outcome; IVW: inverse variance weighted.

It is made available under a [CC-BY 4.0 International license](https://creativecommons.org/licenses/by/4.0/).

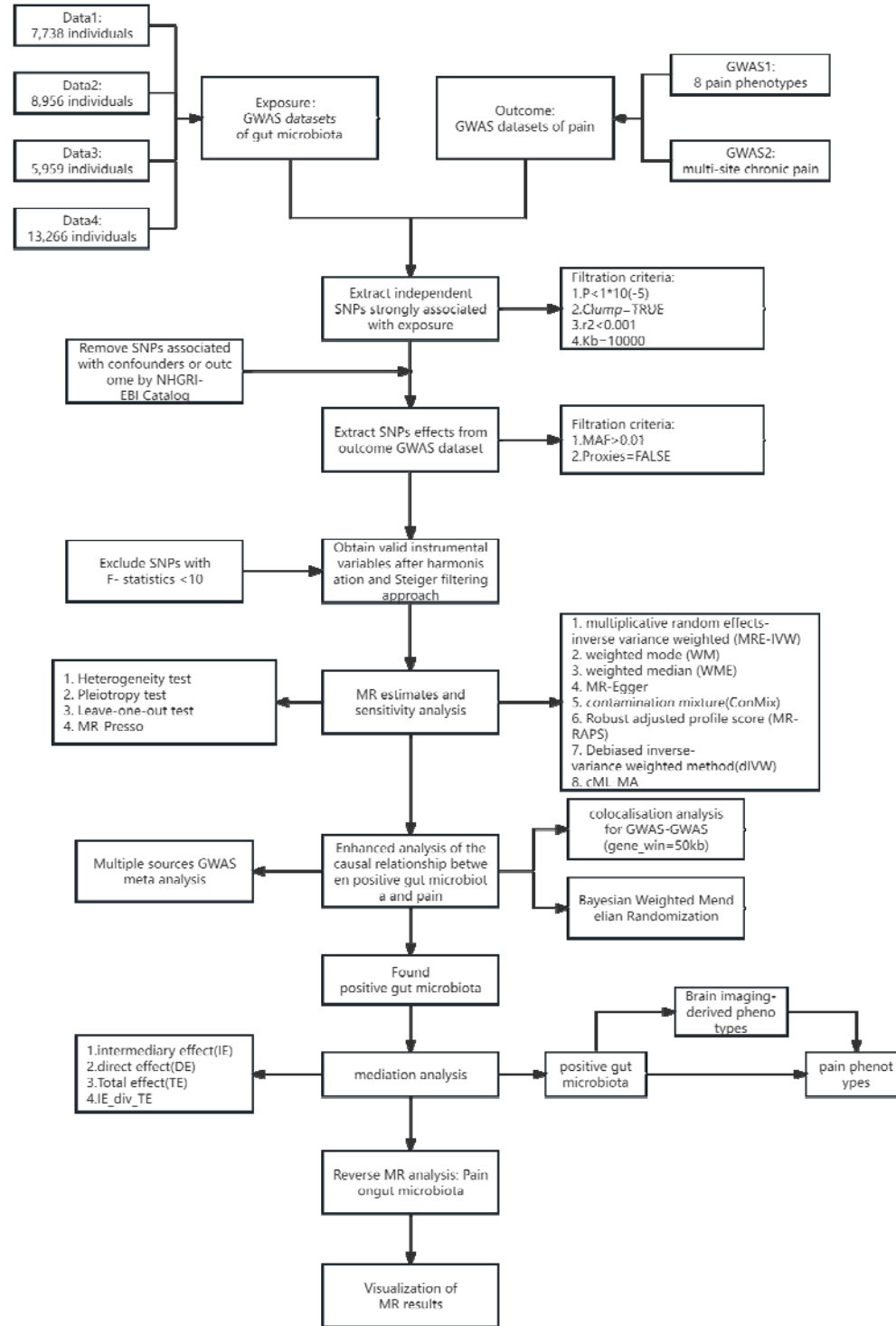


Figure 1: Flow chart of study

It is made available under a [CC-BY 4.0 International license](https://creativecommons.org/licenses/by/4.0/).

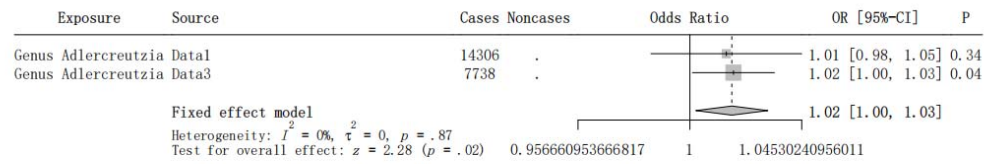


Figure 2a The Forest plots of Meta analysis of Genus Adlercreutzia on MCP

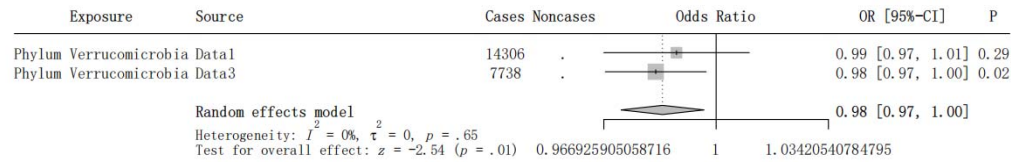


Figure 2b The Forest plots of Meta analysis of Phylum Verrucomicrobia on MCP

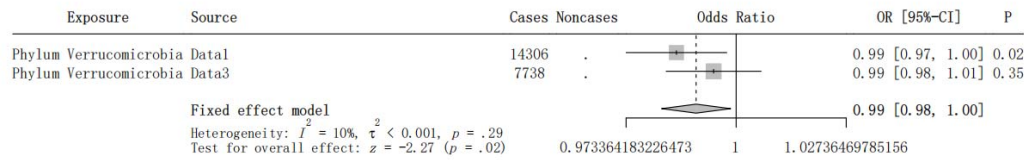


Figure 2c The Forest plots of Meta analysis of Phylum Verrucomicrobia on Headache

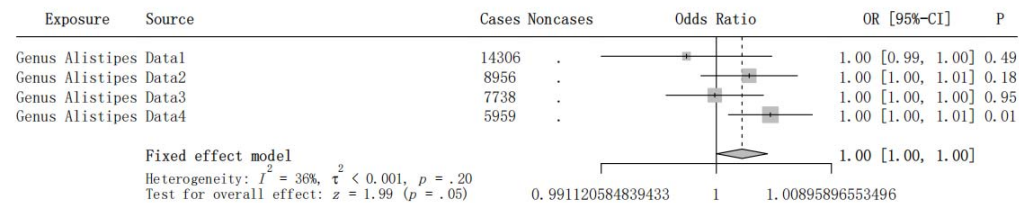


Figure 2d The Forest plots of Meta analysis of Genus Alistipes on Facialpain

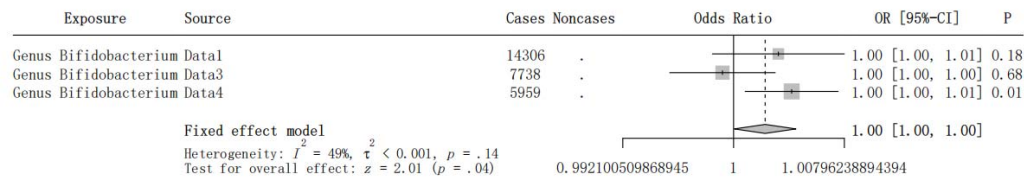


Figure 2e The Forest plots of Meta analysis of Genus Bifidobacterium on Facialpain

It is made available under a [CC-BY 4.0 International license](https://creativecommons.org/licenses/by/4.0/).

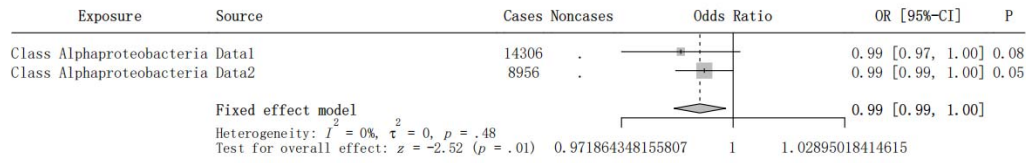


Figure 2f The Forest plots of Meta analysis of Class Alphaproteobacteria on Neckshoulderpain

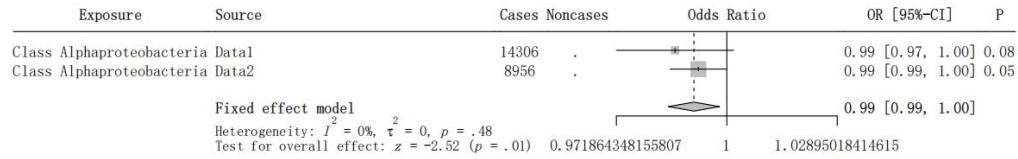


Figure 2g The Forest plots of Meta analysis of Genus Odoribacter on Neckshoulderpain

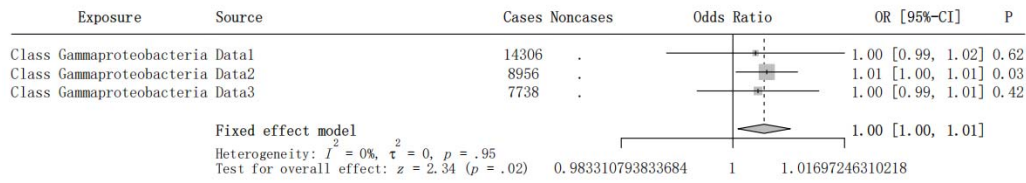


Figure 2h The Forest plots of Meta analysis of Class Gammaproteobacteria on Abdominalpain

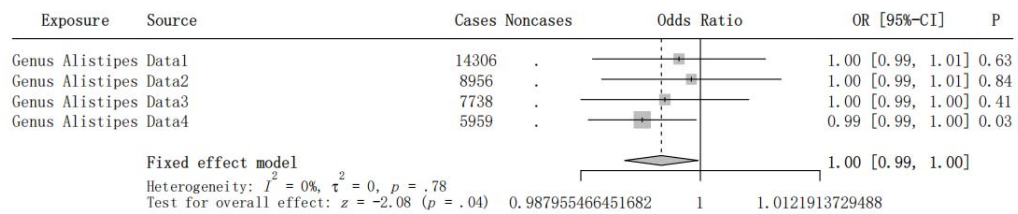


Figure 2i The Forest plots of Meta analysis of Genus Alistipes on Abdominalpain

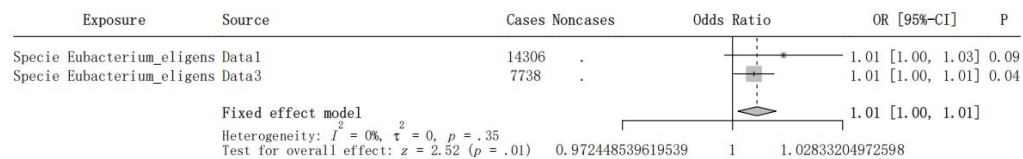


Figure 2j The Forest plots of Meta analysis of Specie Eubacterium_eligens on Abdominalpain

It is made available under a [CC-BY 4.0 International license](https://creativecommons.org/licenses/by/4.0/).

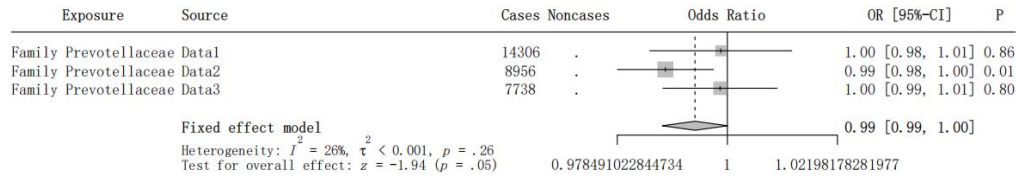


Figure 2k The Forest plots of Meta analysis of Family Prevotellaceae on Backpain

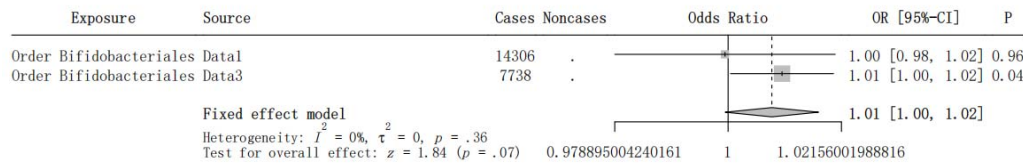


Figure 2l The Forest plots of Meta analysis of Order Bifidobacteriales on Backpain

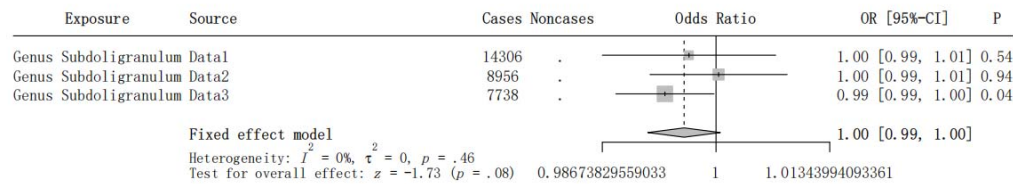


Figure 2m The Forest plots of Meta analysis of Genus Subdoligranulum on Hippain

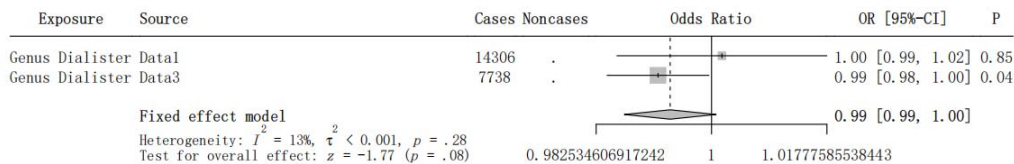


Figure 2n The Forest plots of Meta analysis of Genus Dialister on Kneepain

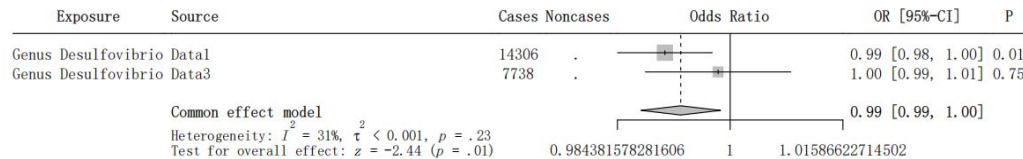


Figure 2o The Forest plots of Meta analysis of Genus Desulfovibrio on pain all over body

It is made available under a [CC-BY 4.0 International license](https://creativecommons.org/licenses/by/4.0/) .

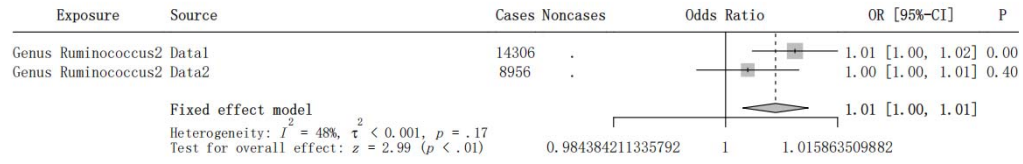


Figure 2p The Forest plots of Meta analysis of Genus Ruminococcus2 on pain all over body

It is made available under a [CC-BY 4.0 International license](https://creativecommons.org/licenses/by/4.0/).

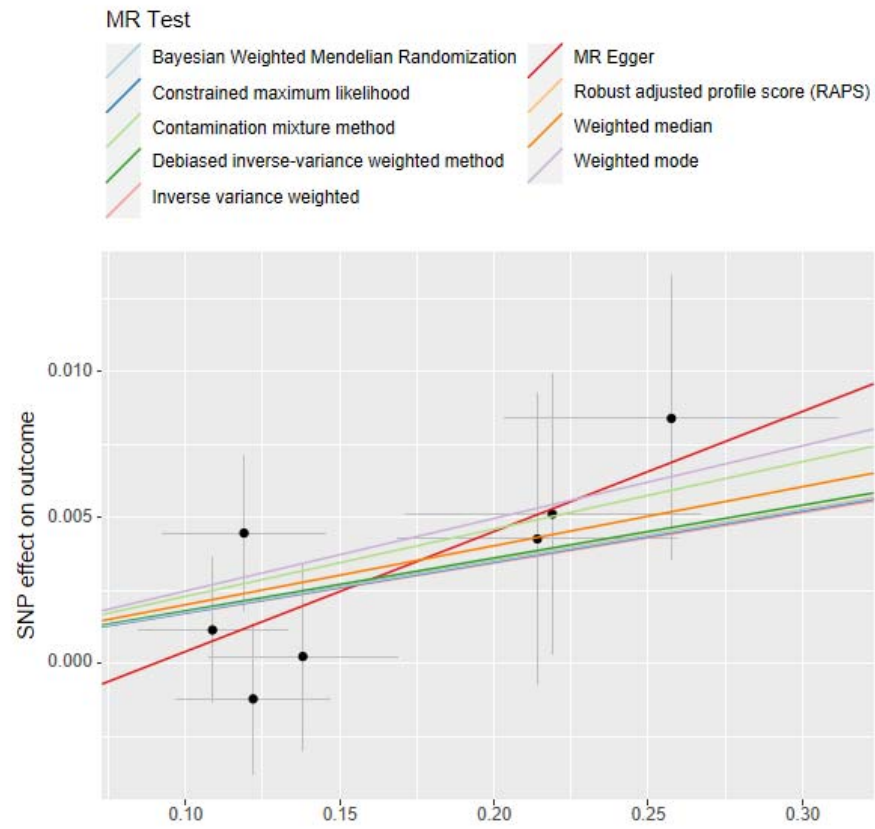


Figure 3a The scatter plots of MR: Genus Adlercreutzia on MCP

It is made available under a [CC-BY 4.0 International license](https://creativecommons.org/licenses/by/4.0/) .

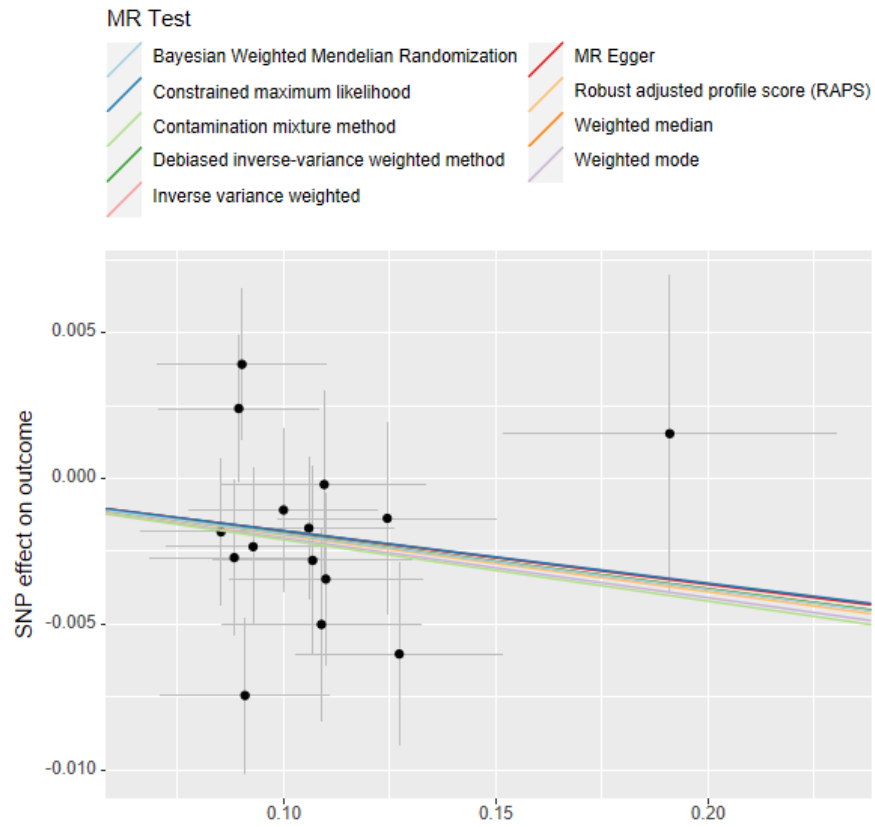


Figure 3b The scatter plots of MR: Phylum Verrucomicrobia on MCP

It is made available under a [CC-BY 4.0 International license](https://creativecommons.org/licenses/by/4.0/) .

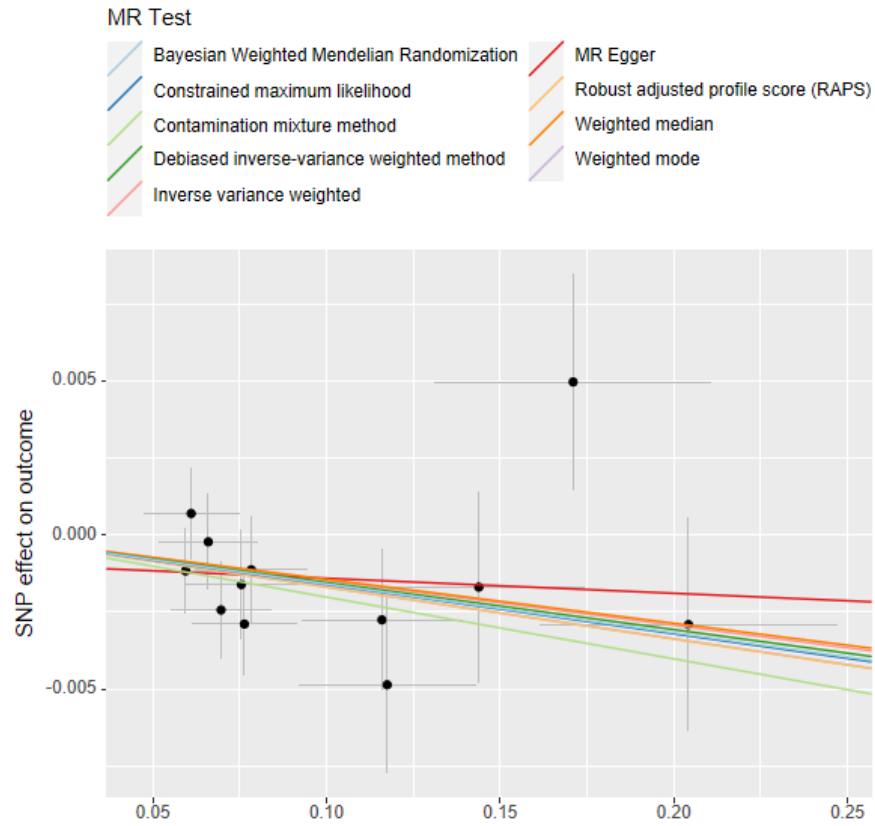


Figure 3c The scatter plots of MR: Phylum Verrucomicrobia on Headache

It is made available under a [CC-BY 4.0 International license](https://creativecommons.org/licenses/by/4.0/).

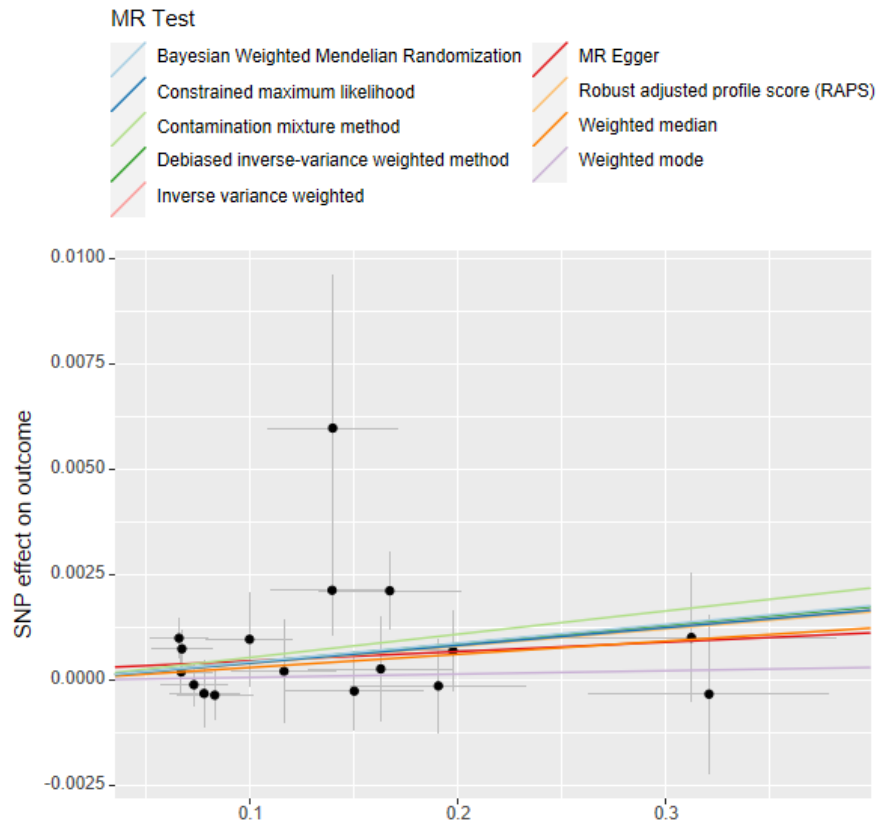


Figure 3d The scatter plots of MR: Genus Alistipes on Facialpain

It is made available under a [CC-BY 4.0 International license](https://creativecommons.org/licenses/by/4.0/).

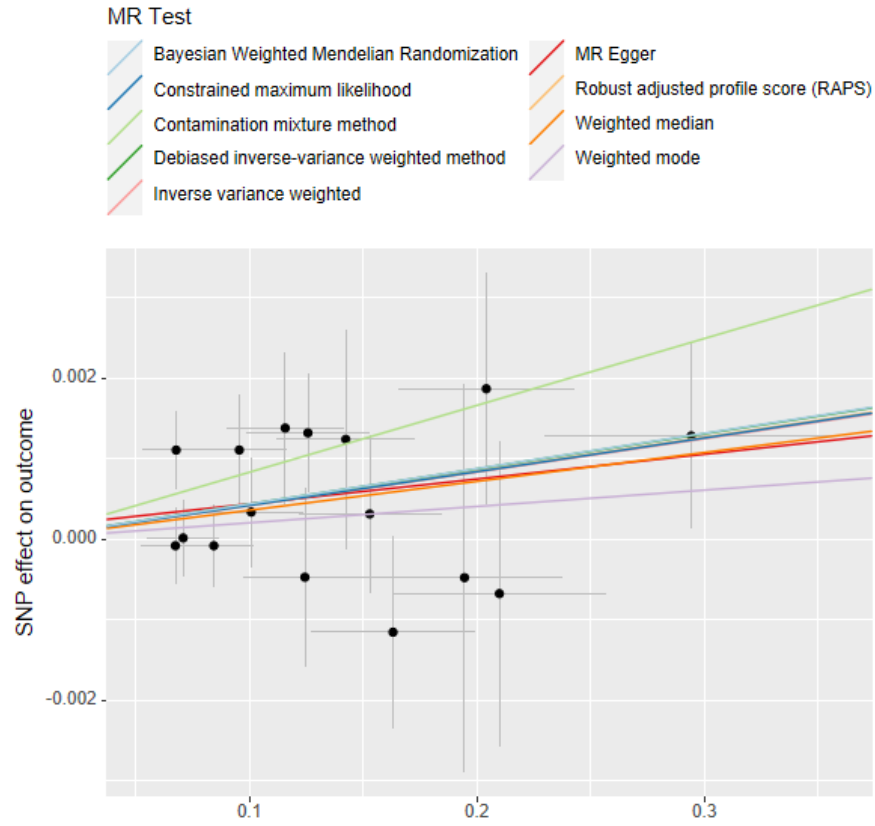


Figure 3e The scatter plots of MR: Genus Bifidobacterium on Facialpain

It is made available under a [CC-BY 4.0 International license](https://creativecommons.org/licenses/by/4.0/) .

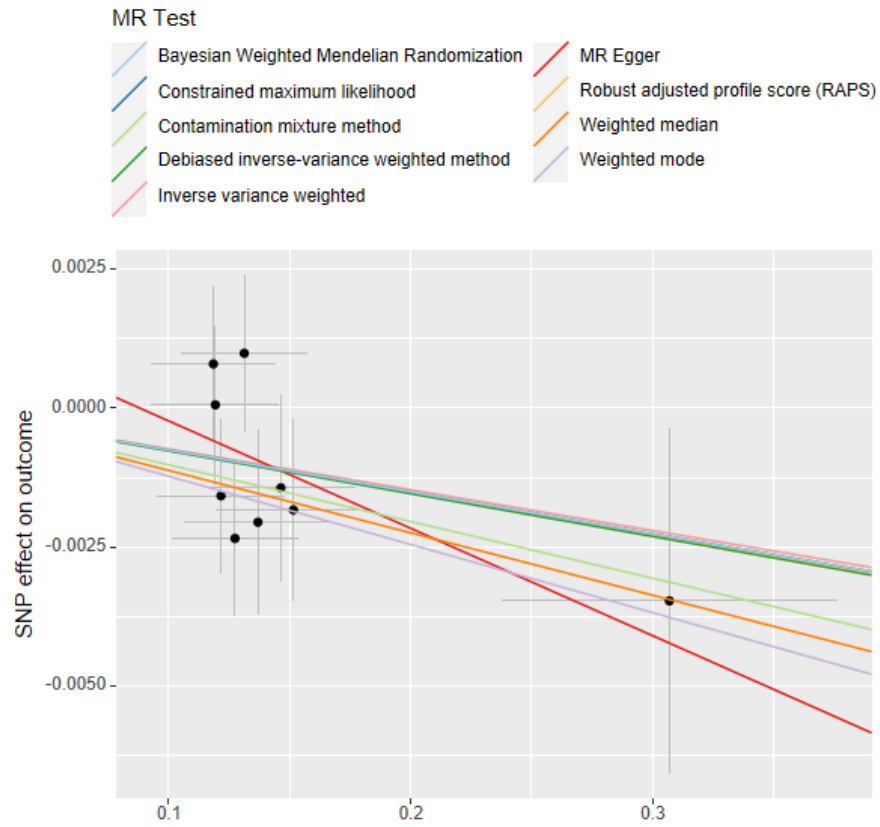


Figure 3f The scatter plots of MR: Class Alphaproteobacteria on Neckshoulderpain

It is made available under a [CC-BY 4.0 International license](https://creativecommons.org/licenses/by/4.0/).

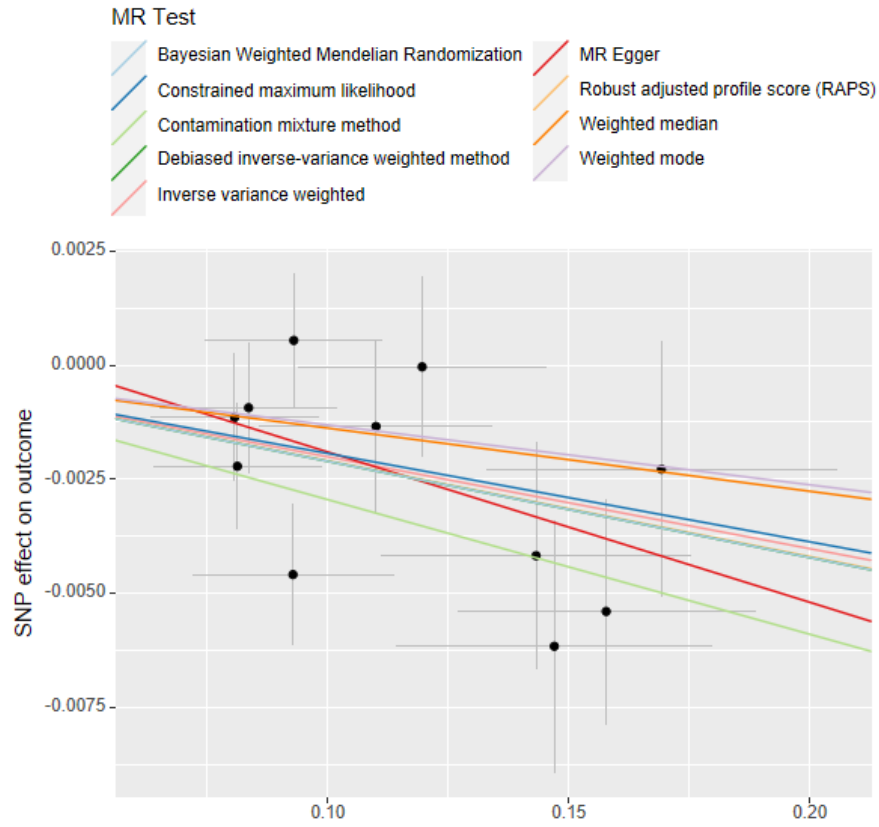


Figure 3g The scatter plots of MR: Genus Odoribacter on Neckshoulderpain

It is made available under a [CC-BY 4.0 International license](https://creativecommons.org/licenses/by/4.0/) .

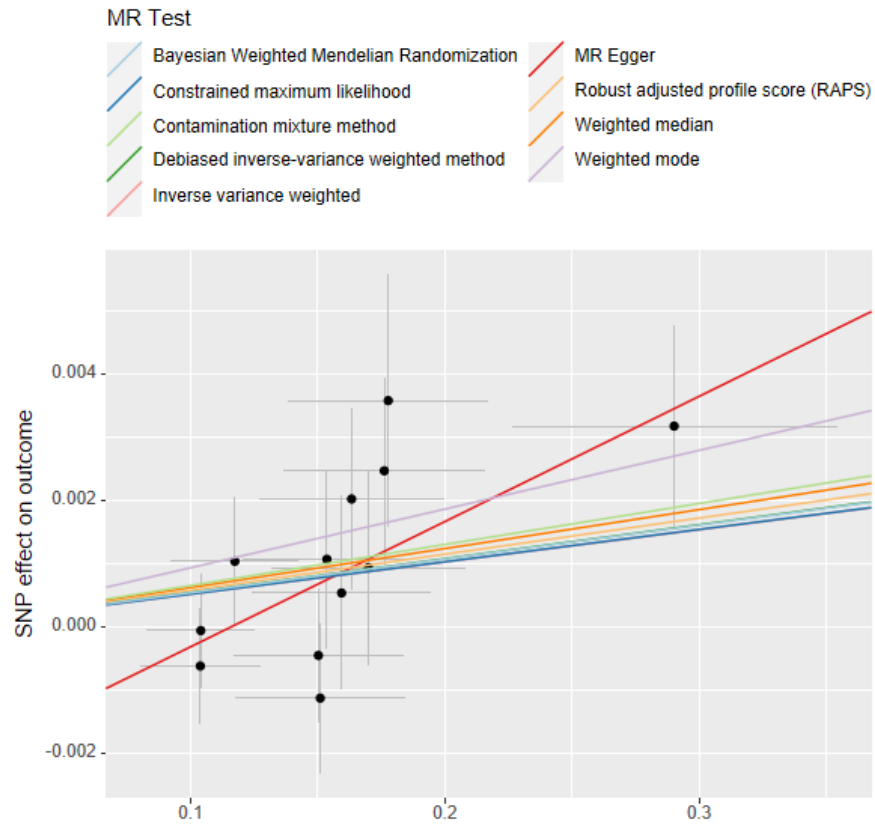


Figure 3h The scatter plots of MR: Class Gammaproteobacteria on Abdominalpain

It is made available under a [CC-BY 4.0 International license](https://creativecommons.org/licenses/by/4.0/).

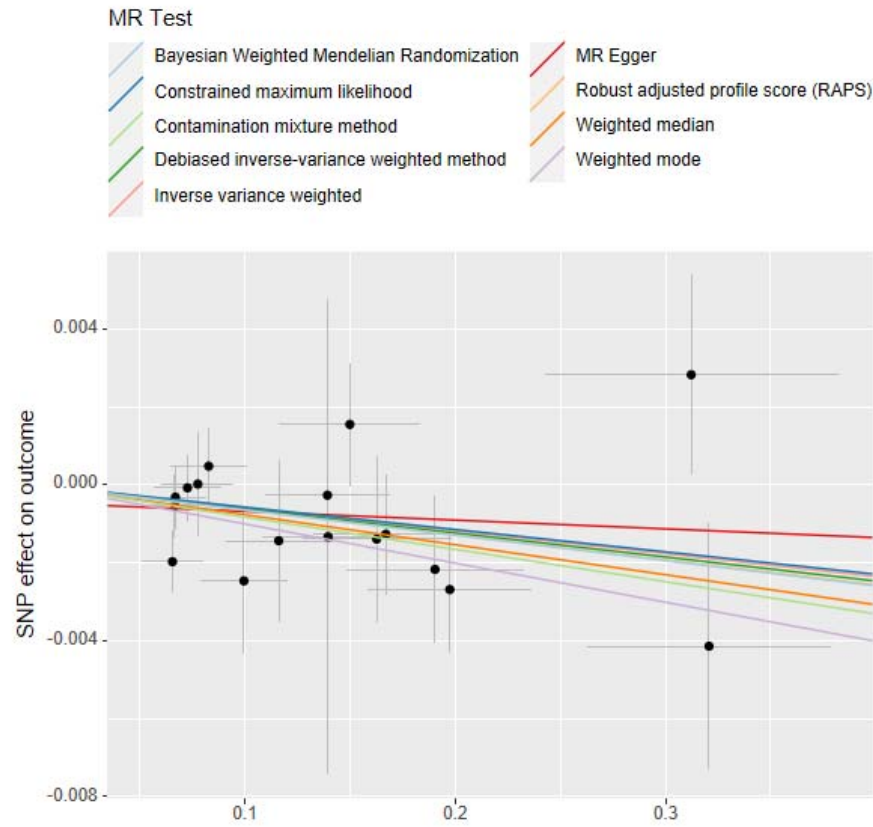


Figure 3i The scatter plots of MR: Genus Alistipes on Abdominalpain

It is made available under a [CC-BY 4.0 International license](https://creativecommons.org/licenses/by/4.0/).

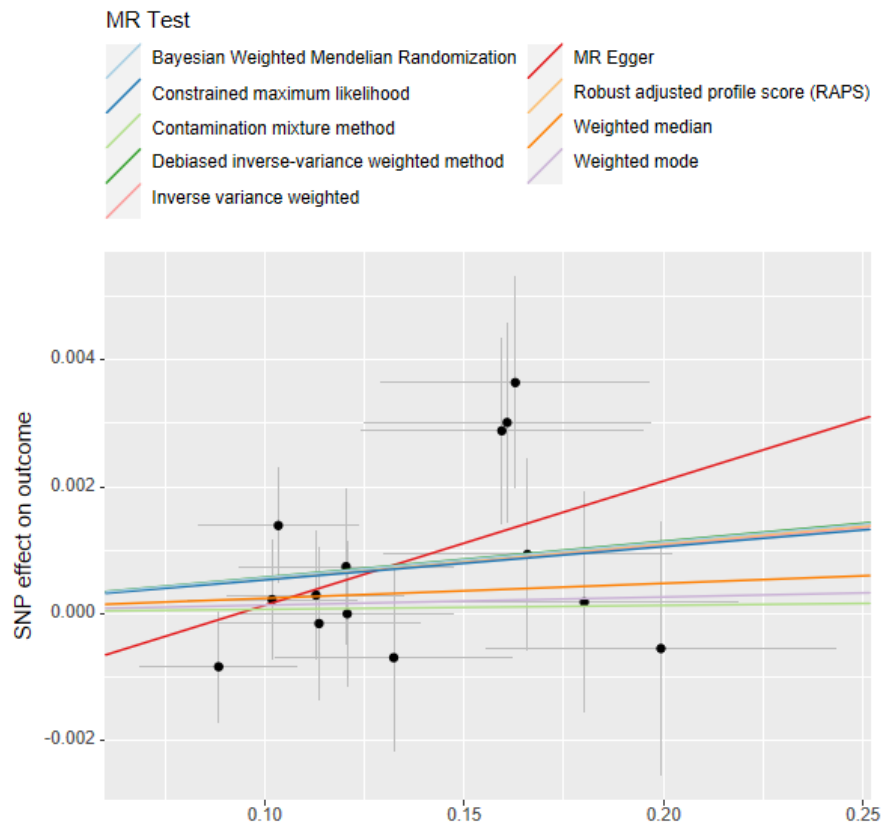


Figure 3j The scatter plots of MR: Specie Eubacterium_eligens on Abdominalpain

It is made available under a [CC-BY 4.0 International license](https://creativecommons.org/licenses/by/4.0/).

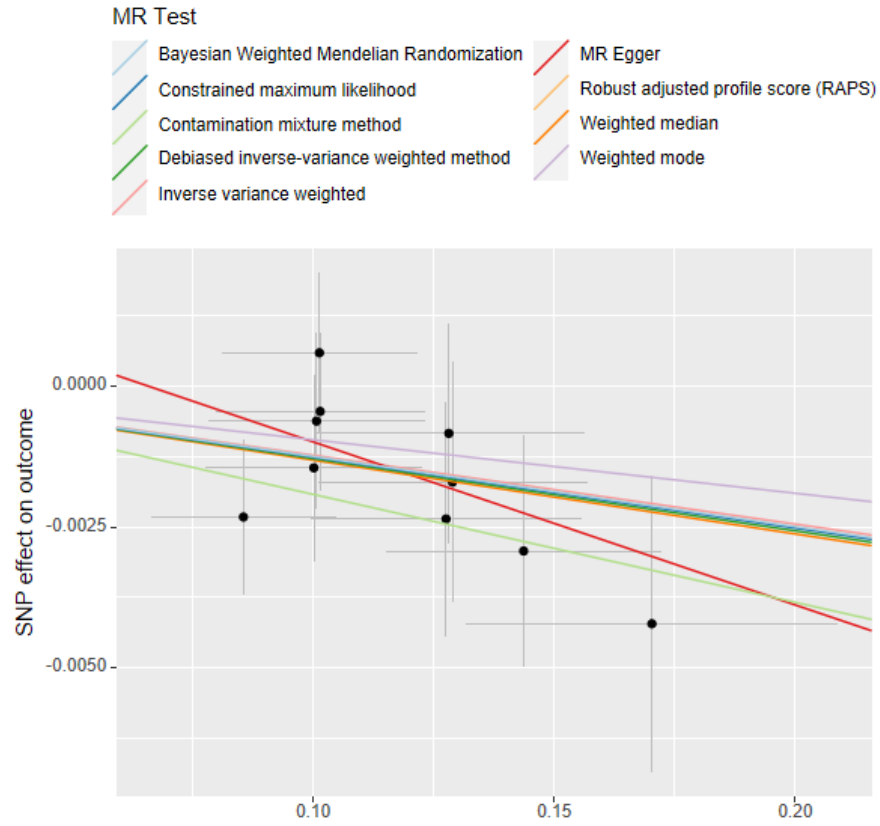


Figure 3k The scatter plots of MR: Family Prevotellaceae on Backpain

It is made available under a [CC-BY 4.0 International license](https://creativecommons.org/licenses/by/4.0/).

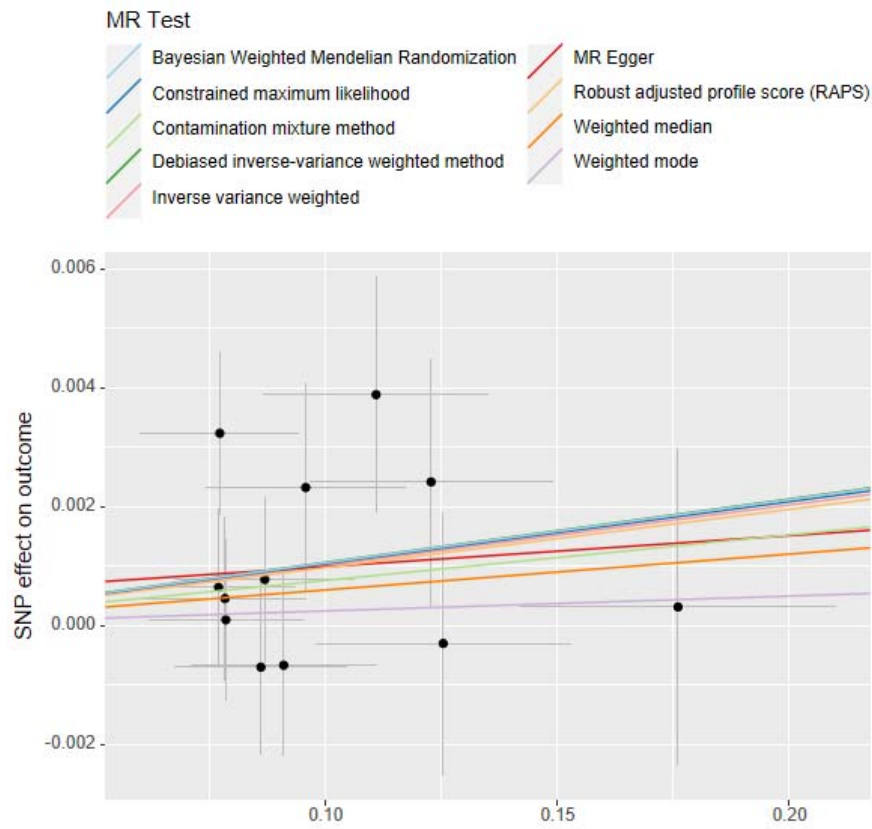


Figure 3| The scatter plots of MR: Order Bifidobacteriales on Backpain

It is made available under a [CC-BY 4.0 International license](https://creativecommons.org/licenses/by/4.0/).

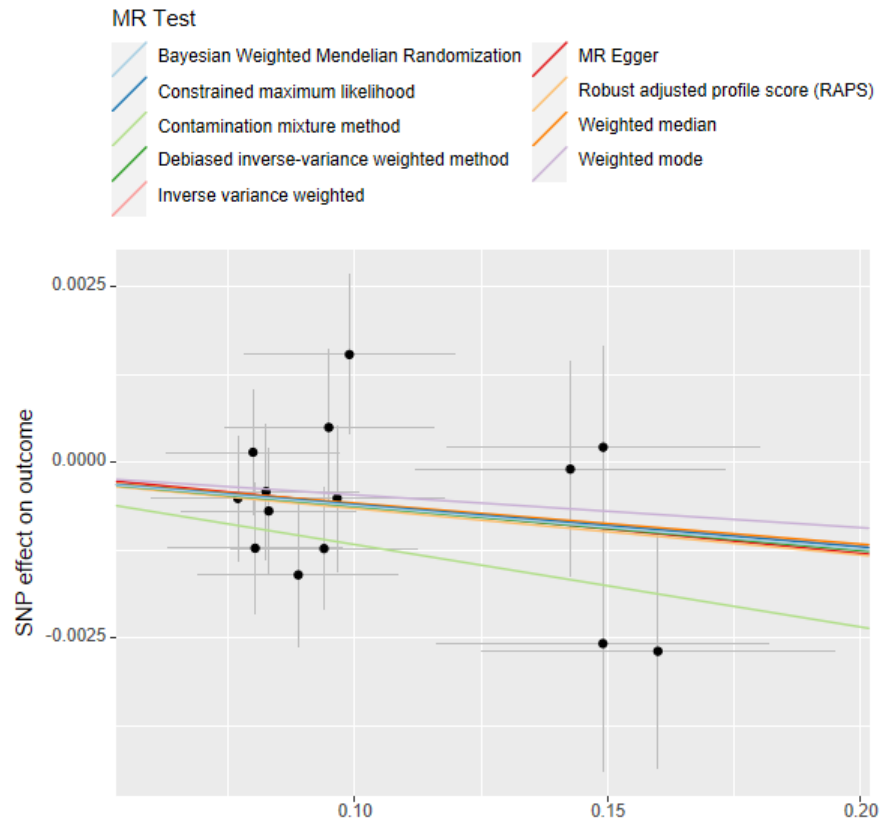


Figure 3m The scatter plots of MR: Genus Subdoligranulum on Hippain

It is made available under a [CC-BY 4.0 International license](https://creativecommons.org/licenses/by/4.0/).

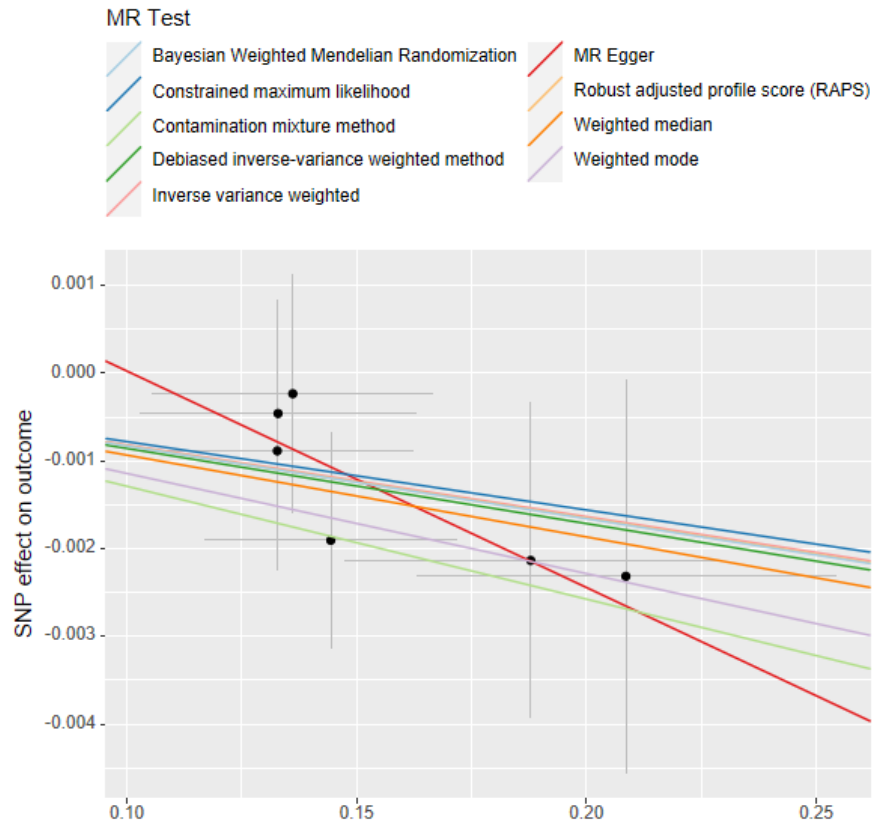


Figure 3n The scatter plots of MR: Genus Dialister on Kneepain

It is made available under a [CC-BY 4.0 International license](https://creativecommons.org/licenses/by/4.0/) .

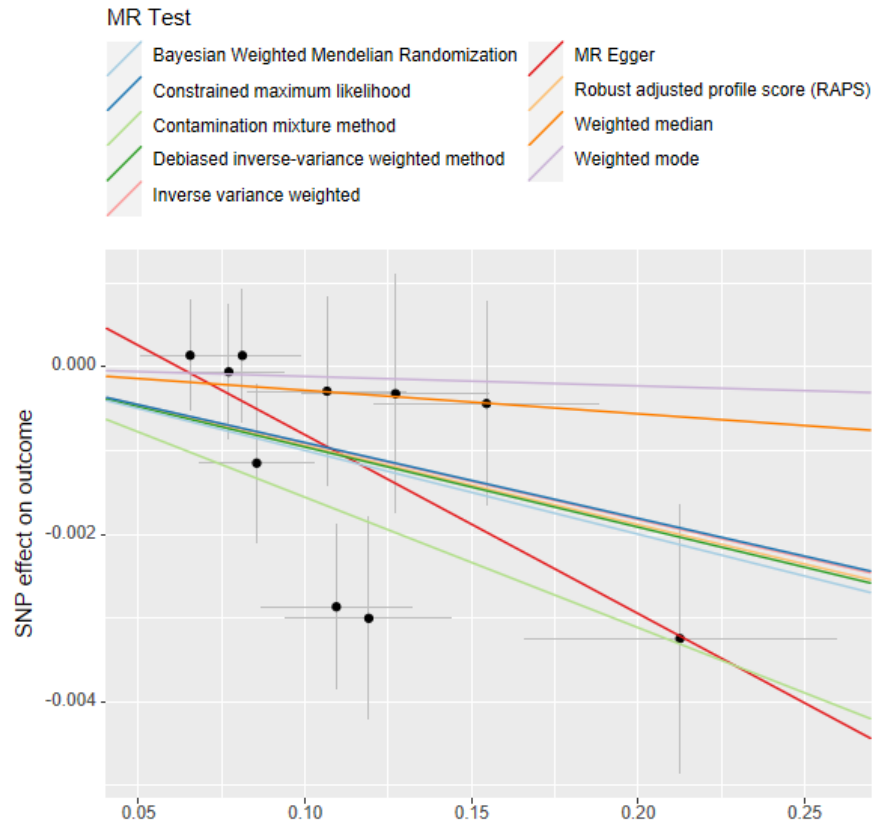


Figure 3o The scatter plots of MR: Genus Desulfovibrio on pain all over body

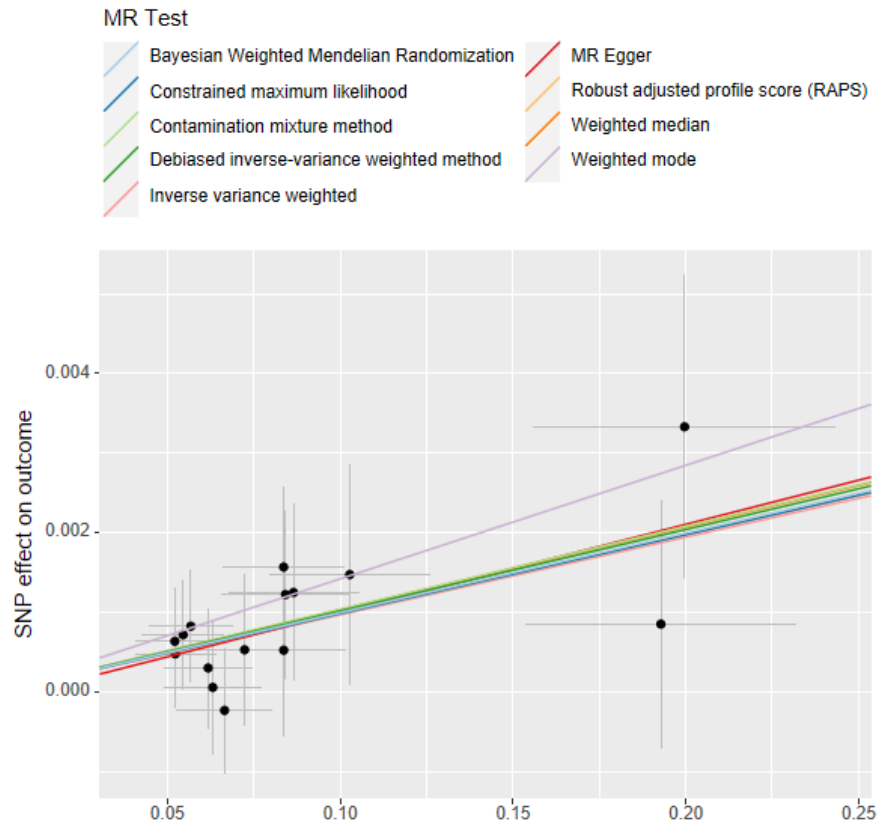


Figure 3p The scatter plots of MR: Genus Ruminococcus2 on pain all over body

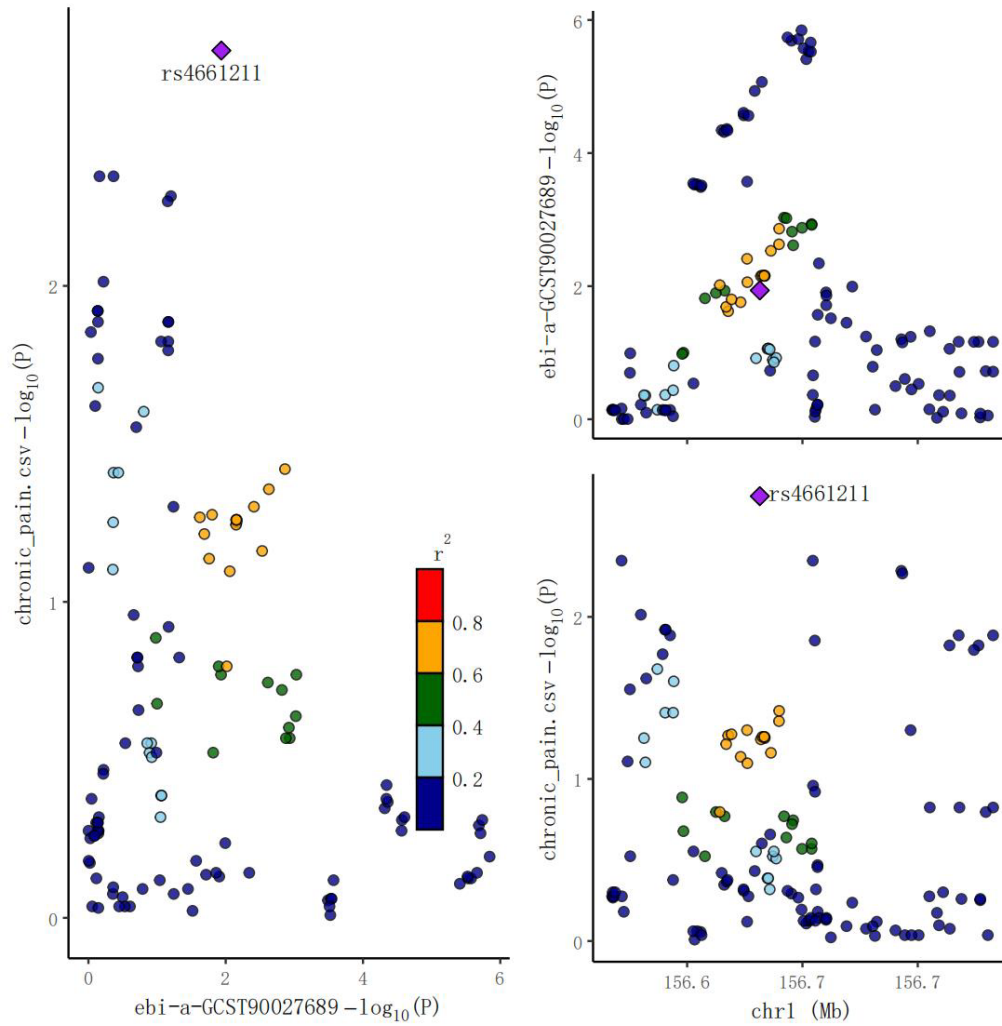


Figure 4a The locuscomparer plot of coloc analysis: Genus Adlercreutzia on MCP

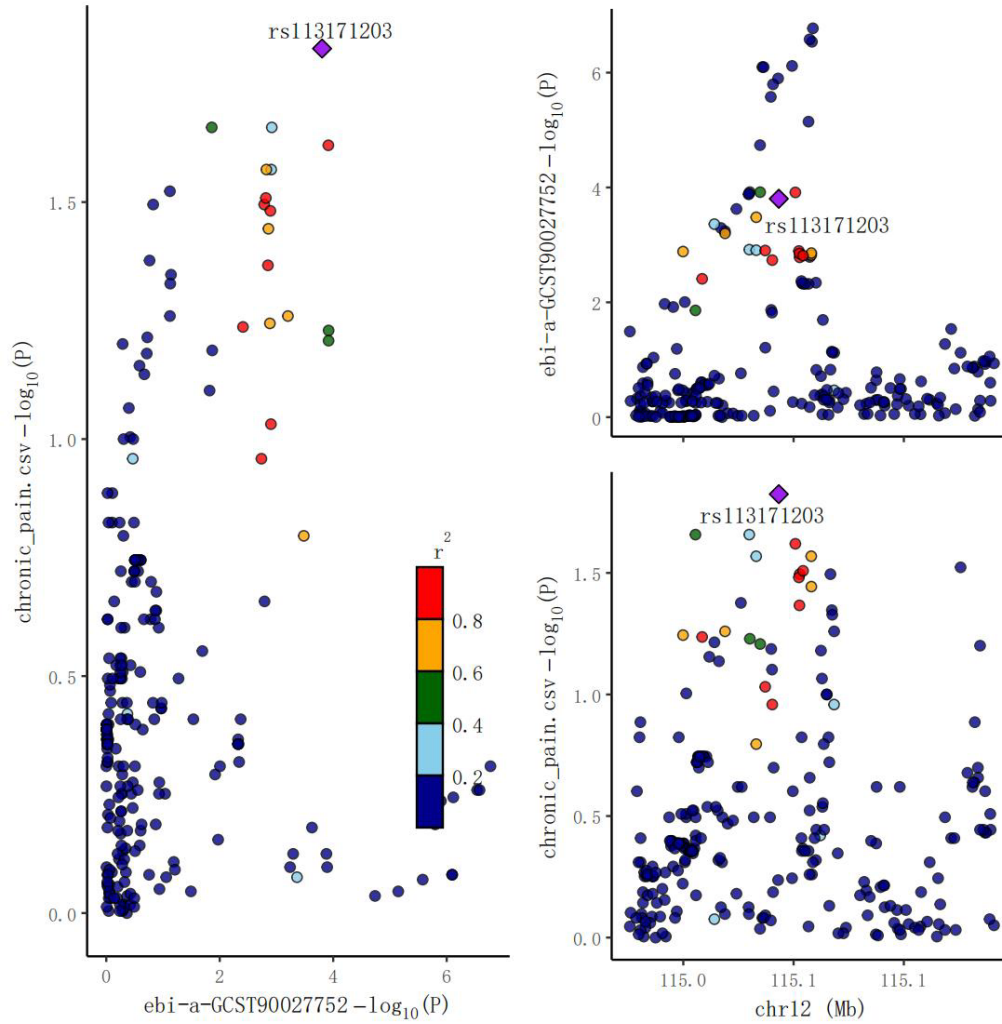


Figure 4b The locuscomparer plot of coloc analysis: Phylum Verrucomicrobia on MCP

It is made available under a [CC-BY 4.0 International license](https://creativecommons.org/licenses/by/4.0/).

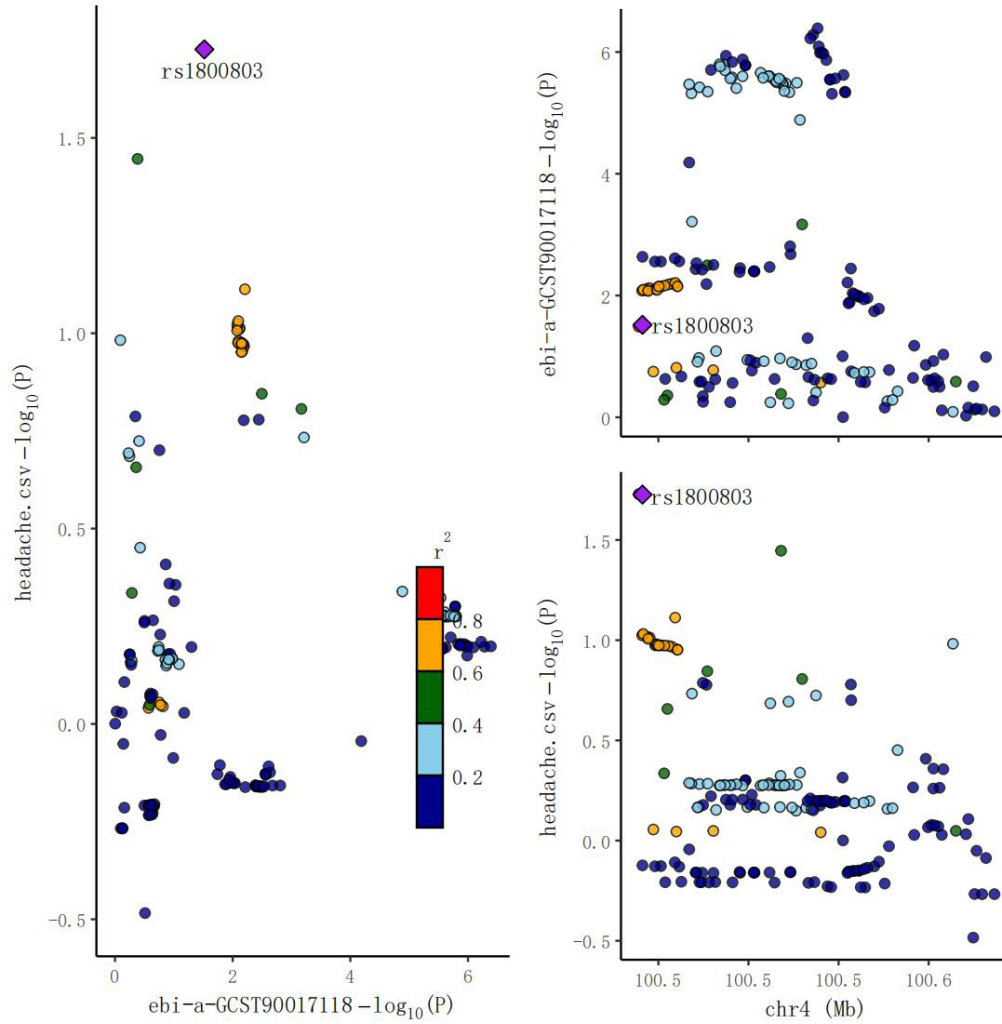


Figure 4c The locuscomparer plot of coloc analysis: Phylum Verrucomicrobia on Headache

It is made available under a [CC-BY 4.0 International license](https://creativecommons.org/licenses/by/4.0/).

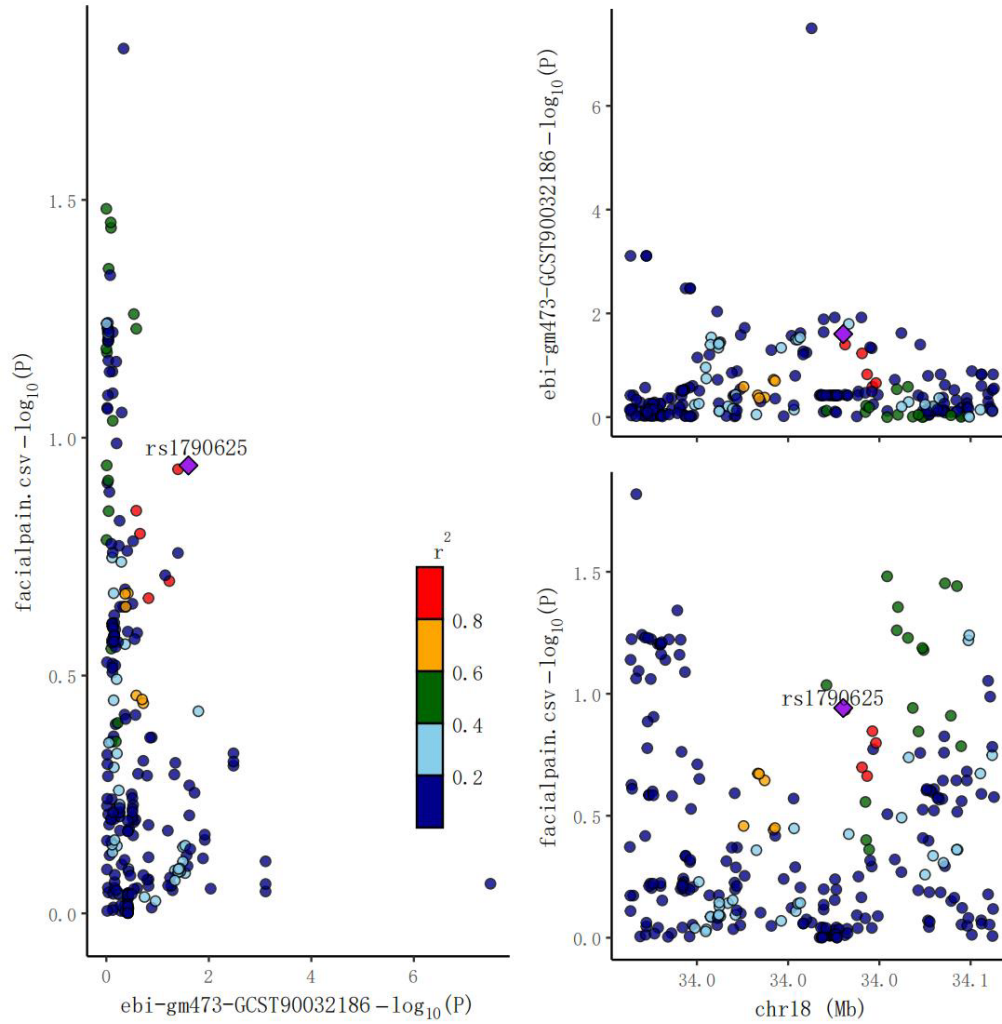


Figure 4d The locuscomparer plot of coloc analysis: Genus Alistipes on Facialpain

It is made available under a [CC-BY 4.0 International license](https://creativecommons.org/licenses/by/4.0/).

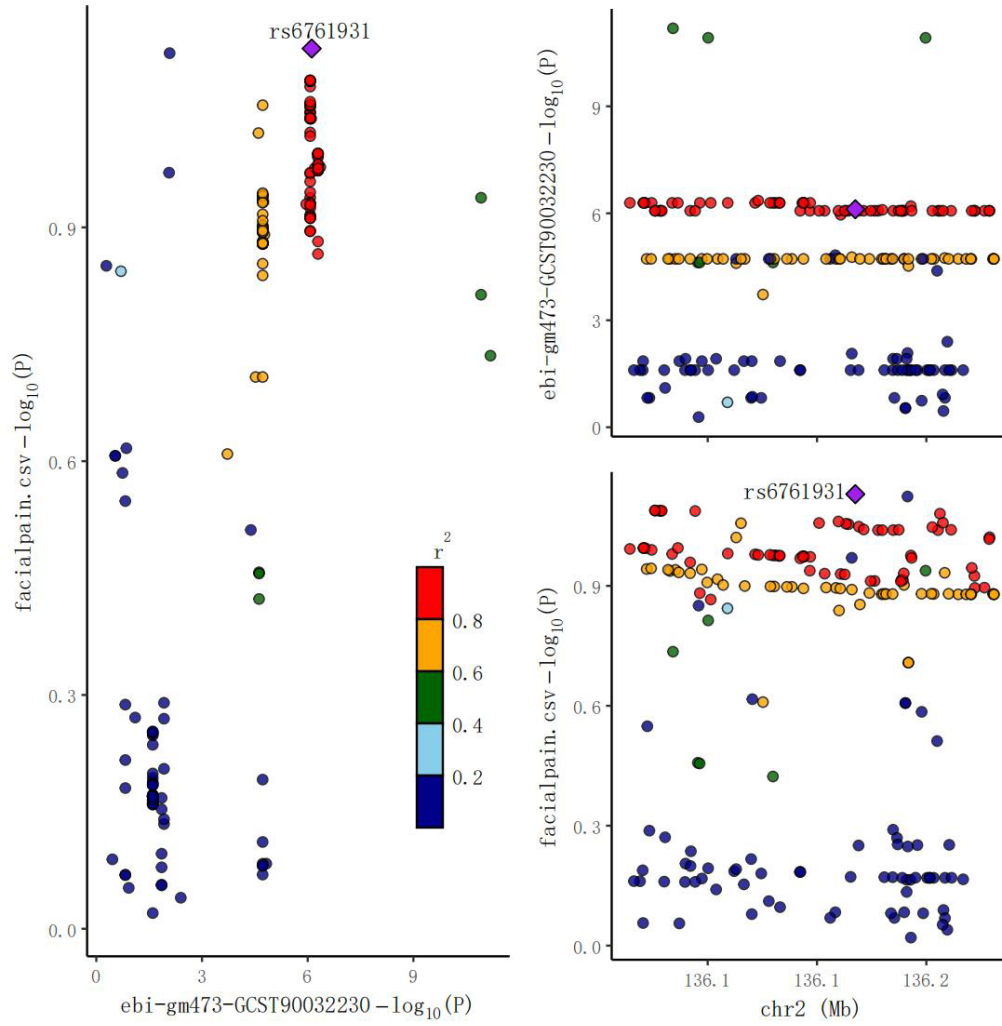


Figure 4e The locuscomparer plot of coloc analysis: Genus Bifidobacterium on Facialpain

It is made available under a [CC-BY 4.0 International license](https://creativecommons.org/licenses/by/4.0/).

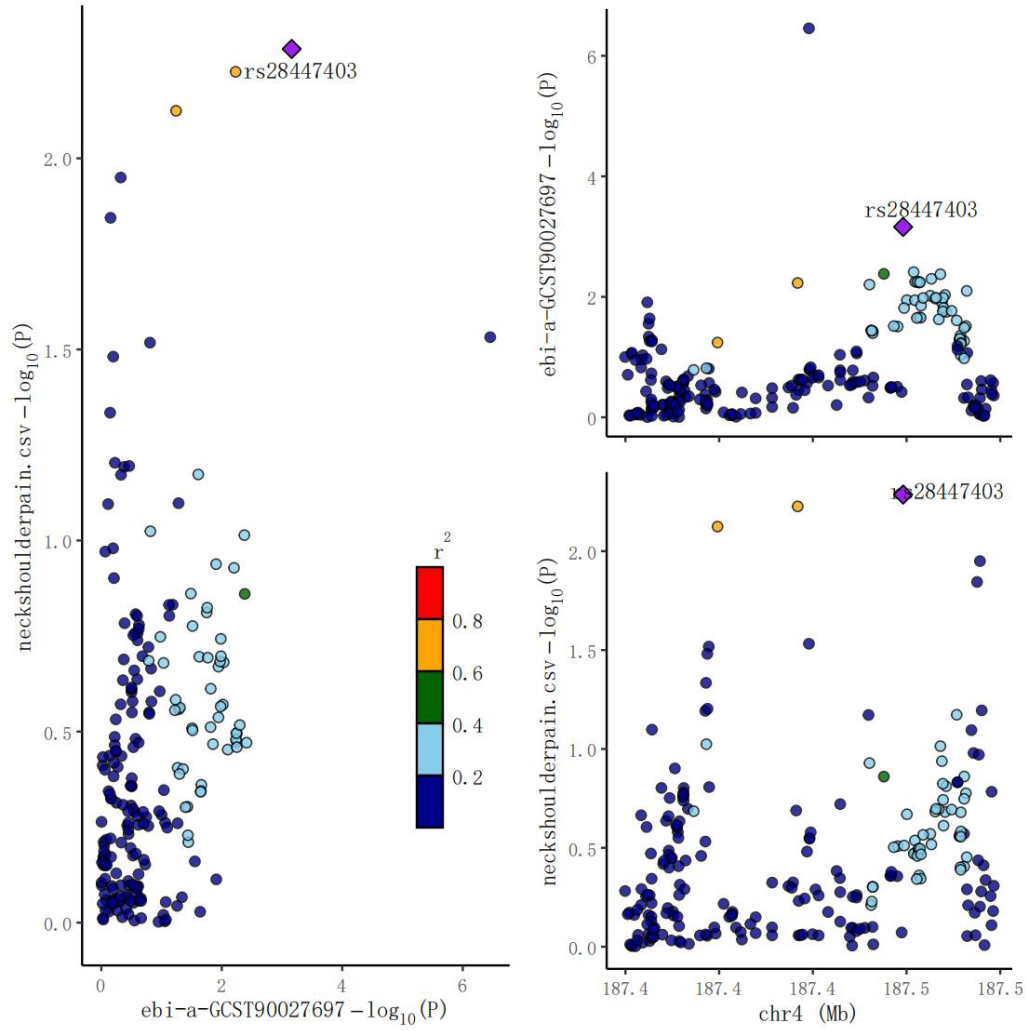


Figure 4f The locuscomparer plot of coloc analysis: Genus *Odoribacter* on Neckshoulderpain

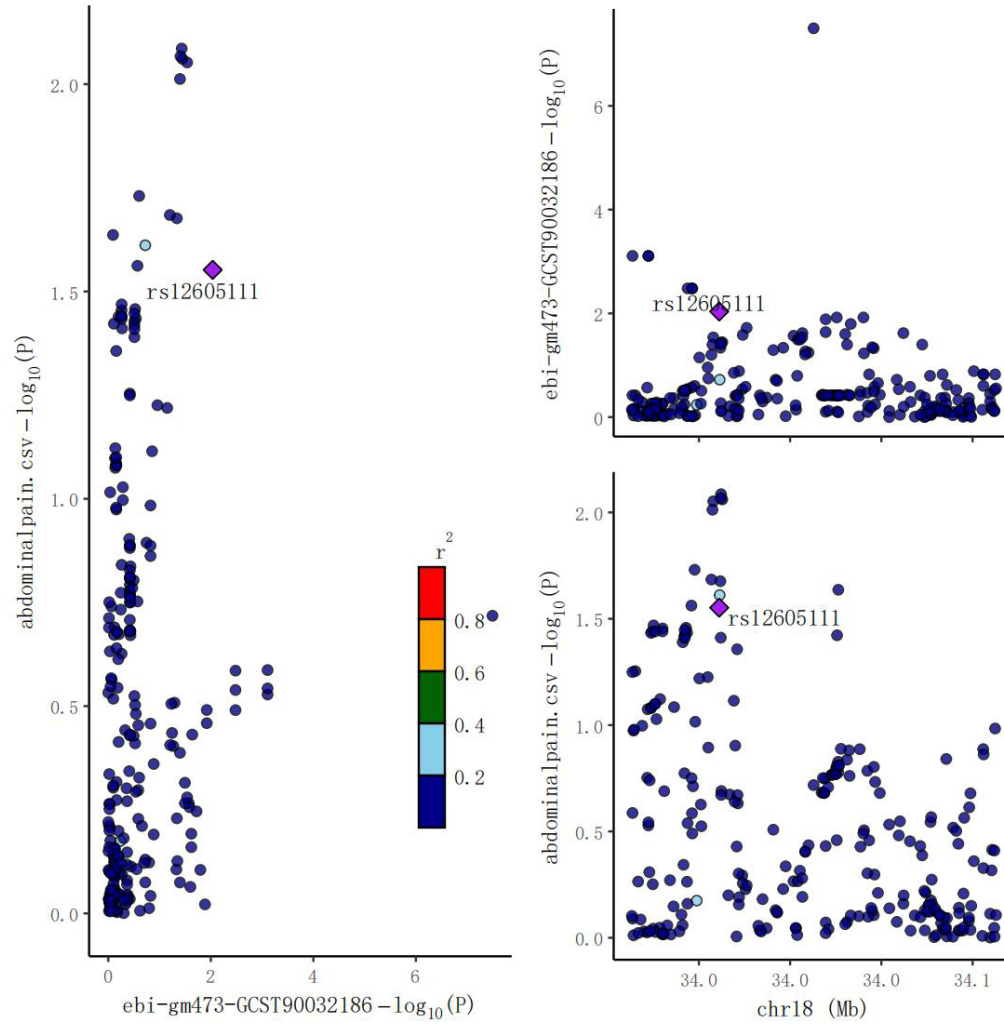


Figure 4g The locus comparison plot of colocalization analysis: Genus *Alistipes* on Abdominalpain

It is made available under a [CC-BY 4.0 International license](https://creativecommons.org/licenses/by/4.0/).

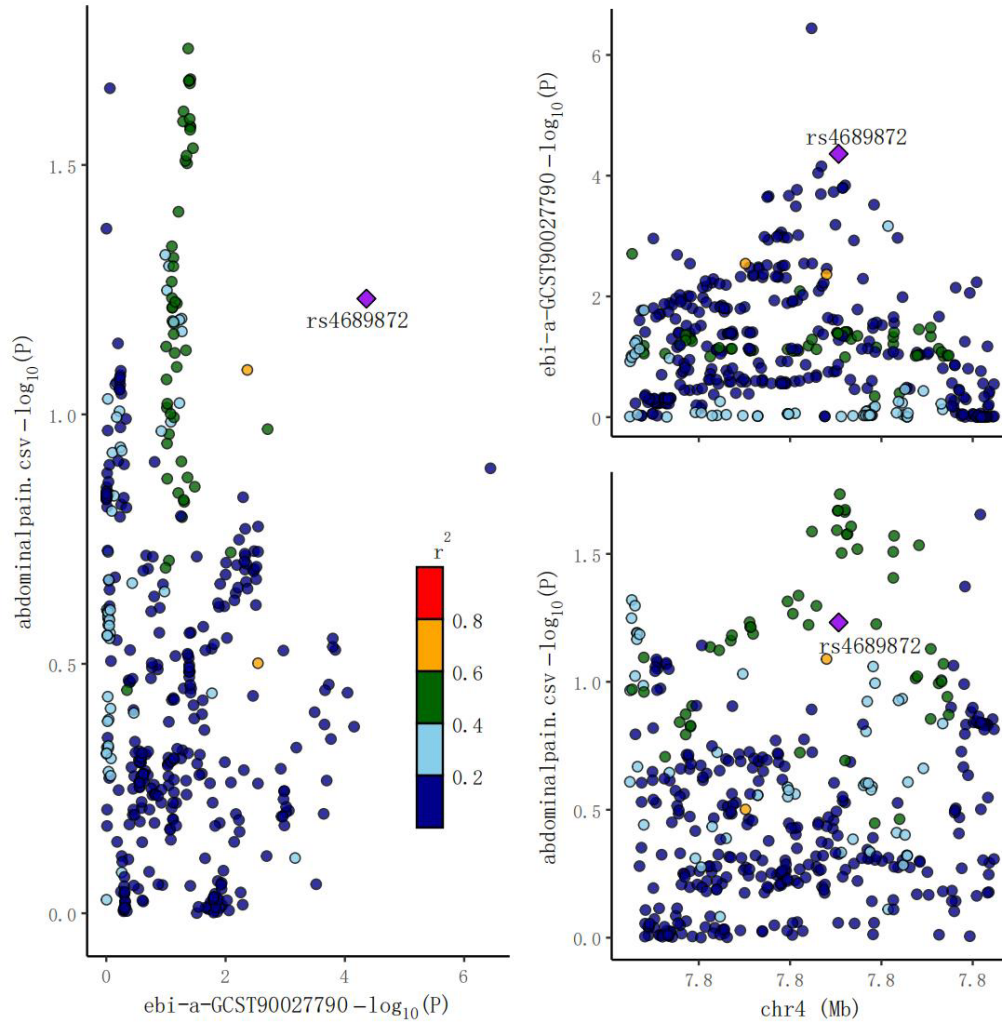


Figure 4h The locuscomparer plot of coloc analysis: Specie *Eubacterium_eligens* on Abdominalpain

It is made available under a [CC-BY 4.0 International license](https://creativecommons.org/licenses/by/4.0/).

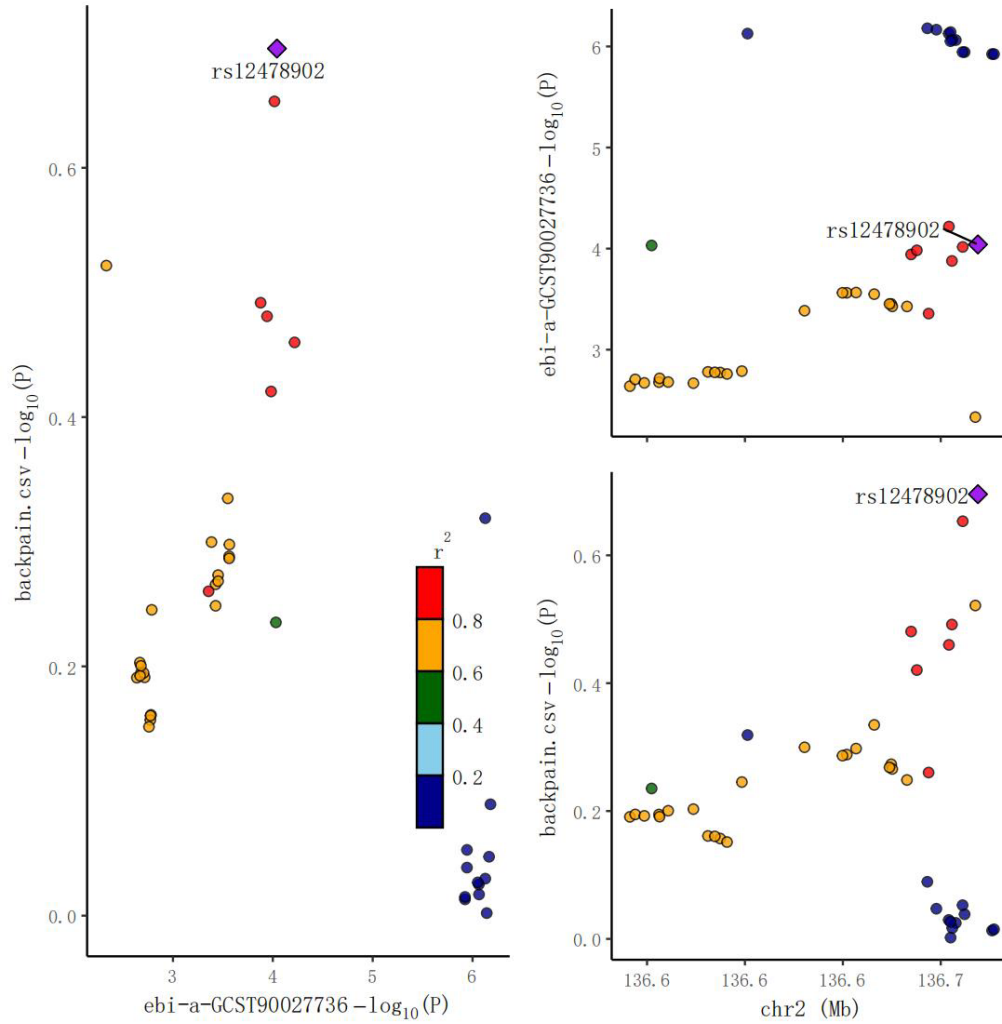


Figure 4i The locuscomparer plot of coloc analysis: Order Bifidobacteriales on Backpain

It is made available under a [CC-BY 4.0 International license](https://creativecommons.org/licenses/by/4.0/).

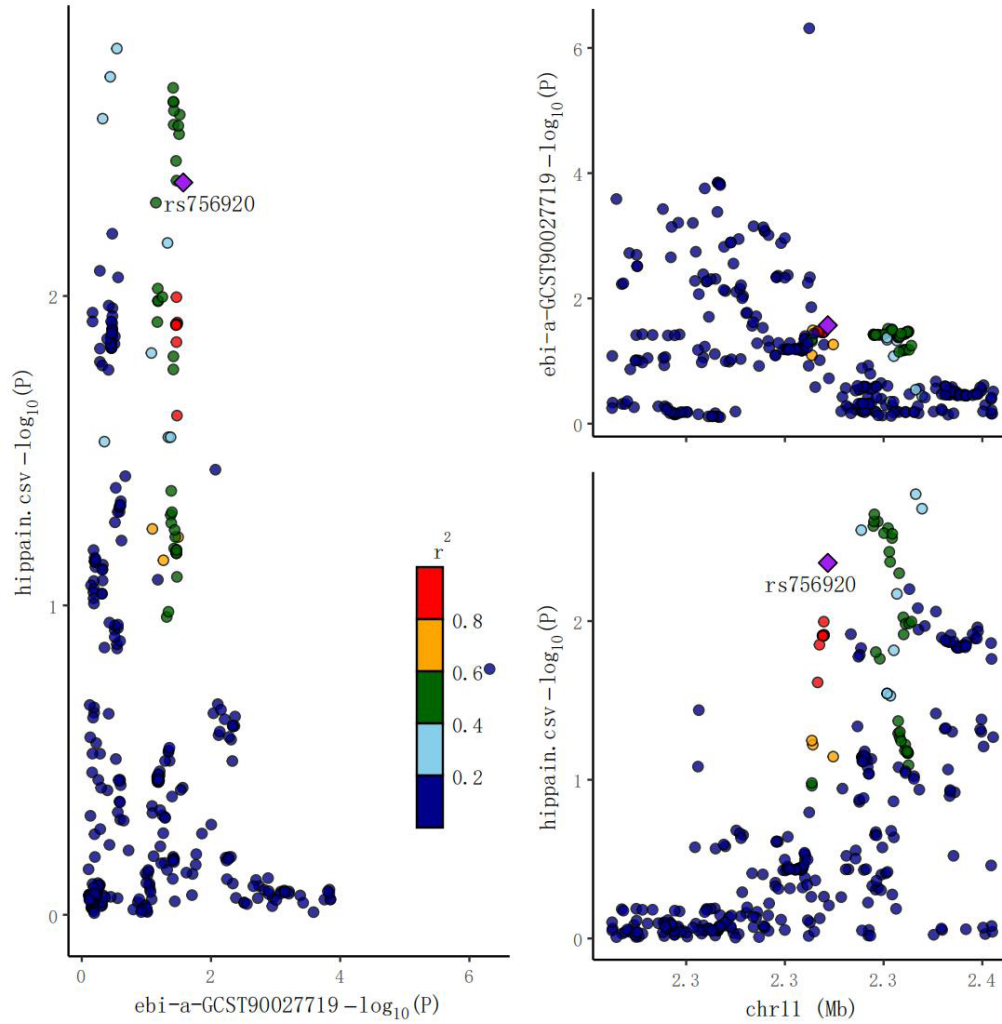


Figure 4j The locuscomparer plot of coloc analysis: Genus Subdoligranulum on Hippain

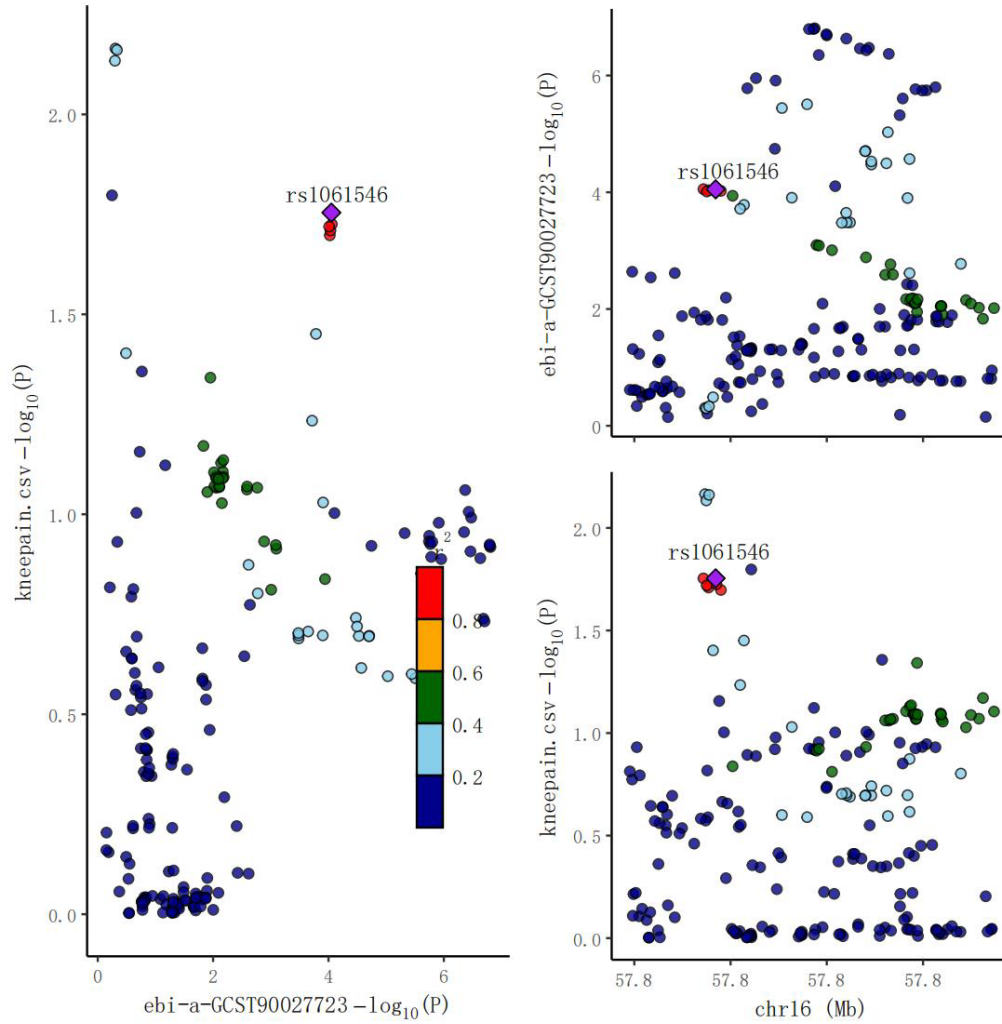


Figure 4k The locuscomparer plot of coloc analysis: Genus Dialister on Kneepain

It is made available under a [CC-BY 4.0 International license](https://creativecommons.org/licenses/by/4.0/).

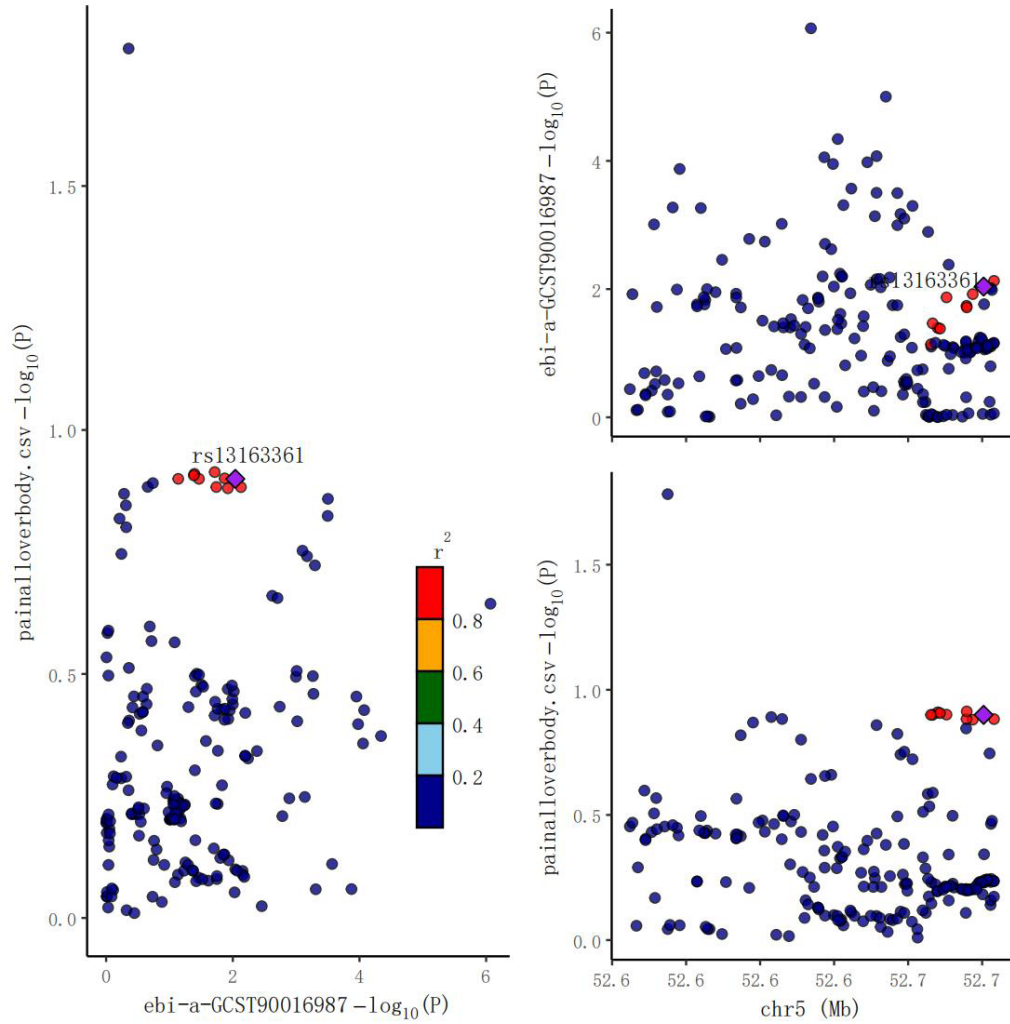


Figure 4| The locuscomparer plot of coloc analysis: Genus *Desulfovibrio* on pain all over body

It is made available under a [CC-BY 4.0 International license](https://creativecommons.org/licenses/by/4.0/).

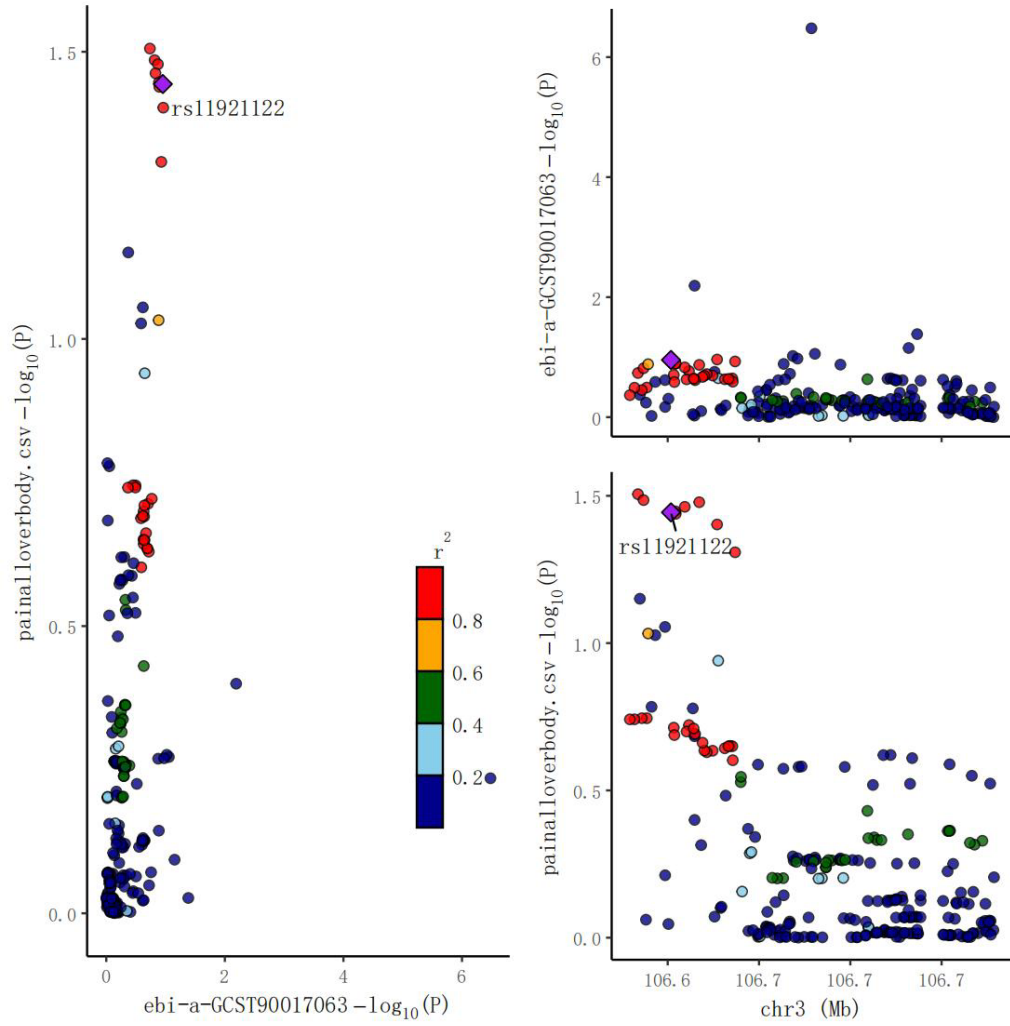


Figure 4m The locuscomparer plot of coloc analysis: Genus Ruminococcus2 on pain all over body

It is made available under a [CC-BY 4.0 International license](https://creativecommons.org/licenses/by/4.0/).

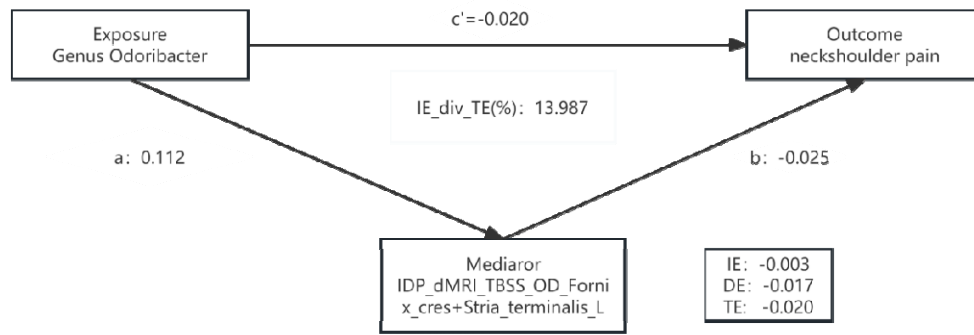


Figure 5 Mediator model: Genus Odoribacter to neck/shoulder pain